UCLA
UCLA Previously Published Works

Title

Recent Advances in Designing Electroconductive Biomaterials for Cardiac Tissue Engineering

Permalink

Journal

ISSN

Authors

Ghovvati, Mahsa
Kharaziha, Mahshid
Ardehali, Reza
et al.

Publication Date

DOI

Recent advances in designing electroconductive biomaterials for cardiac tissue engineering

Mahsa Ghovvati[1], **Mahshid Kharaziha**[2], **Reza Ardehali**[3], **Nasim Annabi**[1,4,*]

[1]Department of Chemical and Biomolecular Engineering, University of California - Los Angeles, Los Angeles, CA 90095, USA

[2]Biomaterials Research Group, Department of Materials Engineering, Isfahan University of Technology, Isfahan 84156-83111, Iran

[3]Division of Cardiology, Department of Internal Medicine, David Geffen School of Medicine, University of California – Los Angeles, Los Angeles, CA 90095, USA

[4]Department of Bioengineering, University of California - Los Angeles, Los Angeles, CA 90095, USA
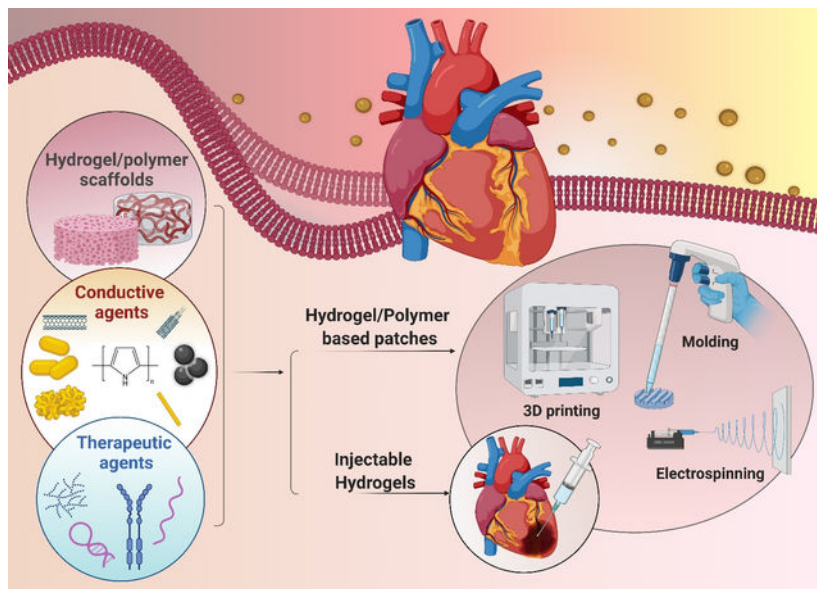
Abstract

Implantable cardiac patches and injectable hydrogels are among the most promising therapies for cardiac tissue regeneration following myocardial infarction (MI). Incorporating electrical conductivity into these patches and hydrogels has been found to be an efficient method to improve cardiac tissue function. Conductive nanomaterials such as carbon nanotubes (CNTs), graphene oxide (GO), gold nanorod (GNR), as well as conductive polymers such as polyaniline (PANI), polypyrrole (PPy), poly(3,4-ethylenedioxythiophene) polystyrene sulfonate (PDOT:PSS) are appealing because they possess the electroconductive properties of semiconductors with ease of processing and have potential to restore electrical signaling propagation through the infarct area. Numerous studies have utilized these materials for regeneration of biological tissues that possess electrical activities, such as cardiac tissue. In this review, we summarize recent studies on the use of electroconductive materials for cardiac tissue engineering and their fabrication methods. Moreover, we highlight recent advancement in developing electroconductive materials for delivering therapeutic agents as one of emerging approaches for treating heart diseases and regenerating damaged cardiac tissues.

Graphical Abstract

*Corresponding author: Prof Nasim Annabi; nannabi@ucla.edu.

Cardiac patches and injectable hydrogels are among the most promising therapies for cardiac tissue regeneration following myocardial infarction. Incorporating electrical conductivity into these patches/hydrogels is an efficient method to improve cardiac tissue function. In this review, recent studies on the use of electroconductive nanomaterials/polymers for cardiac tissue engineering with a particular focus on their application for therapeutic delivery are summarized.

Keywords

cardiac regeneration; conductivity; cardiac patches; injectable hydrogels; drug delivery

1. Introduction

Cardiac diseases remain the leading cause of mortality and disability in the world.[1] It is expected that global mortality related to cardiac diseases increases to 23.6 million by 2030.[2] Myocardial infarction (MI) results from fractional or complete obstruction of coronary arteries. Lack of blood flow to the myocardium may lead to an irreversible loss of cardiomyocytes (CMs), which is replaced by the scar tissue.[3] MI can activate a range of adverse remodeling mechanisms, including arrhythmias, ventricular dilatation, cardiac hypertrophy, and fibrotic scar tissue formation.[4] Scar tissue, formed due to lack of proliferative potential of CMs, is relatively inert and cannot effectively transmit electrical signals and contractile activity, increasing the risk of heart failure.[5] Current therapies for MI include timely revascularization and guideline-directed cardioprotective pharmacotherapy to prevent adverse remodeling and progression of the heart failure.[6] While optimal medical therapy has been used as an effective way to slow the decline in heart function, majority of patients eventually develop heart failure due to irreversible myocardial damage, requiring mechanical circulatory support or heart transplantation. In addition, these strategies suffer from numerous restrictions, including immune rejection, lack of donors, and restricted durability.[7] Recently, regenerative strategies based on stem cell therapy

have shown promising *in vitro* and *in vivo* outcomes.[8] While several clinical trials of cell-based therapy have generated enthusiasm about the potential of stem cells for heart disease, clinical outcomes have been largely inconsistent and no study has yet confirmed the delivery of a pure population of stem/progenitor cells capable of robust cardiac regeneration. [9] Additionally, most of these studies rely on the delivery of exogenous cells into a hostile post-injury cardiac environment, where majority of the transplanted cells die and those that survive do not functionally integrate into the host myocardium. Consequently, it is essential to create innovative strategies which support the infarcted tissue regeneration and repair electromechanical coupling at the site of the dysfunctional heart tissue.

In the past decades, cardiac tissue engineering has been introduced as a promising solution for the construction of off-the-shelf artificial cardiac tissues, which can replace the dysfunctional fragments of the heart after MI.[10] In cardiac tissue engineering, combination of artificial scaffolds, cells, and bioactive molecules are applied to improve the cell-matrix interactions and form a functional cardiac tissue.[11] Many studies have focused on designing biomimetic scaffolds from natural or synthetic materials [12] which can simulate the chemical, mechanical and topographical features of the native heart tissue.[13] These scaffolds should provide mechanical support to the infarcted area and support cellular growth and function as well as their engraftment after transplantation.[14] In addition, the morphological features of the scaffolds, at the multi-scale level, including their porosity, pore size, and geometry should facilitate cell infiltration both *in vitro* and *in vivo*.[15] The aligned surface topography of scaffolds also plays a critical role in directing cardiac tissue maturation and remodeling.[16] Moreover, stiffness and flexibility of the scaffolds, in accordance to the host tissue, are critical for improving cardiac tissue function.[17]

The myocardium is an active and contractile tissue with continuous cycles of polarization and depolarization, which can adjust itself according to hormonal balance and corporeal oxygen demands. Consequently, the applied cardiac tissue engineering strategies should use electroconductive biomaterials to support the electrical conduction and revascularization of the infarct area, leading to improved myocardium regeneration.[18]

Electroconductive materials are categorized into carbon-based materials (e.g. carbon nanotubes (CNTs), graphene-based family and carbon dots), conductive polymers (e.g. polypyrrole (PPy)), ionic liquids, metallic nanomaterials (e.g. gold), and recently introduced biomaterials such as melanins (MELs) and silicon nanowires (SiNWs), which are mainly used for engineering both soft and hard tissues constructs with appropriate mechanical and electrical properties (Figure 1).[19]

Electroconductive materials have been extensively investigated and developed for various biomedical applications over the past few decades. A desirable conductive material should be conductive, biocompatible, biodegradable and non-cytotoxic with suitable mechanical properties and structural integrity.[20] Toxicity of electroconductive nanomaterials especially gold and CNTs have been studies extensively. Gold is known to be a safe and chemically inert.[21] No synergistic or suppressive effects was observed in the presence of gold nanoparticles (AuNPs) (using the acceptable limits of 1 %(w/v)), suggesting that AuNPs do not elicit immune reactions.[21c] In addition, several studies were conducted on the uptake

and potential hazards of CNTs (particularly multi-walled carbon nanotubes (MWCNTs)) to humans and other biological systems.[21b] CNTs have been shown to cause minimal cytotoxicity at high concentrations.[21c] Although there is no exposure standard for CNTs, a recommended exposure limit of 7 μg/m^3 for CNTs is proposed by US national institute for occupational safety and health.[22] CNTs can induce inflammatory and apoptosis responses in human T-cells at higher concentrations. However, MWCNTs are the least toxic among the CNTs, carbon nanofibers, and carbon nanoparticles.[21b] Furthermore, conductive structures based on electroconductive polymers, including PPy, and polyaniline (PANI), may induce some level of cytotoxicity specifically when they are used at high concentrations.[23]

Some classes of electroconductive nanocomposite hydrogels may experience a decrease in their electrical conductivity under deformation due to enhanced distances between conductive nanoparticles (NPs) in their network, limiting their applications for propagating electrical impulses consistently with the contractile properties of the cardiac tissues.[24] In addition, although the introduction of electroconductive materials may significantly promote cardiac muscle regeneration *in vitro*, their long-term clinical and therapeutic applications have not been fully investigated. Preclinical studies, using proper large animal models, are required to confirm their biocompatibility, biodegradability, mechanical characteristics, and long term efficacy.[25]

The exceptional electrical, mechanical, and biological properties of electroconductive biomaterials and their roles in directing various cellular functions and tissue remodeling have been widely reviewed.[26] Our group,[27] along with others,[28] studied the functional behavior of various types of electroactive biomaterials to regulate CM function, signal transition, and cardiac tissue regeneration.

In a recent review article by Esmaeili et al.[29] the applications of electroconductive materials in the engineering of biomimetic and functional cardiac tissues for the treatment of MI was investigated. In addition, Li et al.[18b] recently presented an overview of the types and fabrication methods of conductive biomaterials, and discussed the recent advances in myocardial tissue construction *in vitro* and myocardial repair *in vivo*. However, a comprehensive overview of recently developed electroconductive biomaterials classified based on fabrication methods with a particular focus on their application for therapeutic delivery in cardiac tissue is not yet available.

In the present review, we summarize the latest development of electroconductive materials, in various forms, for *in vitro* and *in vivo* cardiac tissue engineering applications. We provide a brief introduction on the electroconductive properties of the cardiac tissue, followed by a detailed overview of the recently used strategies to develop electroconductive biomaterials for cardiac tissue engineering. Moreover, the ability of electroconductive biomaterials for the delivery of therapeutic agents (e.g. small interfering ribonucleic acid (siRNA), micro ribonucleic acid (miRNA), growth factors, and small molecule inhibitors) for cardiac tissue regeneration are highlighted. Finally, future direction for the design of electroconductive biomaterials for cardiac tissue regeneration are discussed.

2. Cardiac tissue architecture and electroconductivity

The heart wall is made of three layers: the innermost endocardium, myocardium, and the outer epicardium. Within these layers, the compositions of cellular and extracellular matrix (ECM) change according to the functional requirements of that specific area of cardiac tissue. For example, the endocardium is composed of connective tissue, which is supported on one side by a thin layer of endothelium, lining the heart chambers, and on the other side by a layer of smooth muscle fibers that are tangled with the connective tissue. The myocardium's cells are joined to the endocardium by a subendocardial layer. This assembly merges with the heart's conduction system to guide cell signaling and function. Around 33% of the myocardium's cells are CMs, which account for 75% of the heart's volume.[30] In other words, the myocardium consists of precisely positioned CM fibers within connective tissue along with other supporting cells to generate rhythmic cardiac contraction. In addition, other cardiac cell types, including cardiac fibroblasts (CFs), endothelial cells, and mural cells (vascular smooth muscle cells and pericytes), play crucial roles during normal development and pathological conditions.[31] Besides, the ECM also provides structural support to the myofibers and regulates the mechanotransduction of cells, controlling the deposition of structural and functional proteins.[19b] The heart is an electroactive and elastic organ. Its elasticity provides mechanical stability for myocardial relaxation and contraction.[32] The contractility of the healthy heart is related to the regular atrial and ventricular contractions. This process starts in the sinoatrial node (SAN), where pacemaker cells' excitation leads to transmission of signals along a path to the atrioventricular nodes (AVNs) to stimulate atrial contraction. AVN is the slow contractile part of the cardiac conduction system; therefore, this step can preserve the time for ventricles to be filled with blood following the contraction of atria. Other portions of the cardiac conduction system, including conductive bundles and fibers, quickly conduct electrical signals to start the CM depolarization and the final contraction of the ventricles for blood pumping.[33]

The electrophysiological activity of CMs is related to the transfer of charged ions, including sodium, potassium, and calcium, across the cell membrane via regulated channels and receptors. [34] Electrical signal coupling in the cardiac conduction system is related to the cell-cell communications by transferring these ions via structures such as transverse tubules, and intercalated discs, including fascia adherens, desmosomes, and gap junctions. Among them, gap junctions ensure mechanical coupling between CMs and enable propagation of electrical impulses throughout the heart.

In the ischemic heart, CMs are replaced by a stiff and non-contractile scar layer, which can block or delay electrical propagation. This layer can result in turbulences in cell-cell communications and disruption of ion-channel activity, leading to desynchronized contractions and arrhythmia.[35] This cellular and extracellular changes, which induce cardiac electrical weakening, can be treated using elimination of the main activating factors and management of the secondary structural disorders. Consequently, besides drugs and surgeries, regenerative strategies are also helpful for improving the conduction function of the myocardium. In this regard, therapies based on electroconductive biomaterials may be used as a promising cardiac regenerative approach.[36] In the following sections, the role of electroconductive materials on CM function and myocardium regeneration is discussed.

3. Cardiac tissue engineering approaches based on using electroconductive materials

Generally, cardiac tissue regeneration based on the use of electroconductive biomaterials consists of two strategies: i) fabrication of electroconductive patches/scaffolds *in vitro* and their suturing/gluing to the infarcted area, and ii) development of injectable conductive hydrogels and their direct injection to the myocardium. In both approaches, the electroconductive materials are utilized to transmit electrochemical and electromechanical signals and to electrically stimulate CMs, leading to improved cellular function and tissue regeneration. These two platforms can also be applied as a carrier for the delivery of therapeutic agents, genes, and growth factors to promote cell function and neovascularization, and enhance myocardium regeneration. Recent studies on designing various types of electroconductive cardiac patches and injectable hydrogels for cardiac tissue regeneration are described in the following sections.

3.1. Cardiac Patches

One promising technique for cardiac tissue regeneration is the use of cardiac patches.[37] Cardiac patches, also known as two- dimensional (2D) and three-dimensional (3D) heart muscle structures, are tissue-like constructs that can be used to improve contractile function in cases of acute MI.[38] The use of conductive cardiac patches can bypass abnormal areas of failed or slow conduction in the damaged heart to prevent reentrant dysrhythmia and restore normal conduction.[39] In order to integrate successfully with the native tissue, these patches must closely resemble the configuration of the native ECM as well as the heart's electroconductivity.[37] When used as a cell delivery scaffold, the alignment of the CMs in the cardiac patches is essential in order to maintain the microarchitecture and biological functions of the native tissue.[37, 40] Hence, patterning the cardiac patches has been the subject of numerous studies aiming to align CMs and create functional cardiac tissues. To this end, various methods have been used to pattern the polymeric substrates used for CMs alignment, including micropatterning, electrospinning, and 3D printing techniques.[41] In addition, conductive biomaterials have been added to these substrates to further improve CM function and alignment.[42] Matching the mechanical strength of the myocardium is another important property of these engineered cardiac patches. These scaffolds should exhibit remarkable mechanical resilience to withstand repeated cycles of stretching during cardiac beating.[43] For instance, Olvera and colleagues engineered an electroconductive cardiac patch based on polycaprolactone (PCL) coated with *in situ* polymerized PPy.[44] They used a melt electrospinning method to develop an auxetic patch that could accommodate the strains and stresses in the human myocardium during systole and diastole. This auxetic patch also showed anisotropic mechanical properties, mimicking the directionally dependent mechanics of the native myocardium. Moreover, PPy coating provided the electrical properties appropriate for myocardial regeneration. In another study, to evaluate the impact of conductive materials on CMs, Navaei *et al* engineered cardiac patches based on gold nanorod (GNR) incorporated gelatin methacryloyl (GelMA) seeded with CMs.[45] As opposed to pristine GelMA hydrogel structures, CMs interacted with the GNRs within the designed cardiac patch, which resulted in substantially faster and synchronous electrical signal propagation. Furthermore, their results showed an improved

local alignment of F-actin fibers at high concentration of GNRs (i.e., 1 & 1.5 mg/ml). In another study, highly stretchable auxetic patches based on chitosan (CS) and PANI were designed for MI treatment using a rat model.[46] This auxetic design gave the cardiac patch a negative Poisson's ratio, which could mimic the mechanical behavior of the native heart tissue.

3D printing and electrospinning methods are commonly used for fabricating cardiac patches. [37, 39, 43a, 47] Due to inherent differences in these fabrication processes, the resulting patches have shown different thread and pore sizes. Although 3D-printed scaffolds are typically composed of arranged materials with microscale threads and large pores, electrospun sheets are composed of mainly randomly oriented nanoscale threads with much smaller pores. Regardless of their distinctions, both architectures have shown significant effectiveness in generating functional cardiac tissue construct.[48] Table 1 summarizes electroconductive patches designed for cardiac tissue engineering in the recent years with their fabrication method, reported conductivity, and the outcome after applying them *in vitro* and/or *in vivo*.

3.1.1. Engineering cardiac patches using electrospinning—Electrospinning was

first used in cardiac tissue engineering by Shin *et al.* to produce nanofibrous PCL patches seeded with neonatal rat cardiomyocytes (NRCMs).[49] After this initial study, electrospinning was widely used in the fabrication of electroconductive materials for cardiac regeneration.[50] For instance, Hosoyama and co-workers developed a nanocomposite electroconductive collagen (Col)-based cardiac patch for the treatment of the infarcted myocardium.[47a] They prepared an aligned nano-Col fibrous (AF) layer (conductive layer) by electrospinning a Col solution containing AuNPs. The collected nanofibers were then anchored onto an elastic Col hydrogel layer (elastic layer), and the resulting patch was glued to the infarcted myocardium using fibrin glue (Figure 2A(i)). A representative macro image of the engineered electroconductive cardiac patch incorporating AuNPs is shown in Figure 2A(ii). The results of their *in vitro* study showed that these patches were able to increase connexin 43 (Cx43) expression in NRCMs cultured under electrical stimulation and could recover cardiac function. The *in vivo* data using mouse MI model exhibited that only AuNPs -containing patches were able to restore the heart function. Histological analysis also exhibited that blood vessel density and Cx43 levels were increased, and the scar size was reduced in mice that underwent experimental MI and were treated by the patches containing AuNPs. Moreover, fractional area change (FAC), a representative index of myocardial contraction, was improved only for animals that received the implants containing AuNPs (Figure 2A(iii)). Similarly, the results of echocardiography indicated that implantation of the composite material containing AuNPs significantly improved left ventricular ejection fraction (LVEF) as compared to all other groups (Figure 2A(iv)). Furthermore, representative images of Masson-Trichrome (MT) staining of the mice hearts at day 28 post-implantation demonstrated that only the group treated with the cardiac patch containing AuNPs showed a significant decrease in the scar size of ~ 25% (Figure 2A(v)).

In another study, our team developed adhesive and conductive fibrous cardiac patches by electrospinning of GelMA accompanied by the conjugation of an acrylated choline-based bio-ionic liquid (Bio-IL) (Figure 2B).[43a] These cardiac patches were optimized to mimic the conductivity and mechanical properties of the native myocardium. Figure 2B(i)

represents a schematic illustration of electrospinning of GelMA fibrous sheet followed by addition of acrylated Bio-IL prior to ultraviolet (UV)-crosslinking to form the adhesive cardiac patches. In addition, the electrostatic forces between the negatively charged surface of cardiac tissue and positively charged acrylated Bio-IL, as well as covalent bonds between NH_2 functional groups in cardiac tissue and methacrylate groups of GelMA provided a firmly adhesion of the patch to the murine myocardium, eliminating the need for suturing (Figure 2B(ii & iii)). Also, quantification of the adhesion strength of cardiac patches fabricated with 10 % (w/v) GelMA and varying concentrations of acrylated Bio-IL on heart tissue confirmed that the patches containing increased concentrations of acrylated Bio-IL had higher adhesion strength to the heart tissue (Figure 2B(iv)). In addition, the cardiac patches fabricated with varying GelMA and Bio-IL concentrations demonstrated enhanced electrical conductivity by increasing acrylated Bio-IL concentrations (Figure 2B(v)).

Although among different techniques, electrospinning appears to be the simplest but promising method for the fabrication of fibrous cardiac patches,[51] one challenge is to induce fiber alignment. In many applications, a scaffold composed of aligned nanofibers is ideal, as anisotropy in topography and shape can significantly affect both mechanical strength and various cellular functions including adhesion, proliferation, and alignment. [52] In particular, aligned fibrous scaffolds replicate the ECM in the heart tissue, where the ventricular myocardium is made up of perpendicularly interwoven Col stripes. The directional dependence of electrical and mechanical properties of cardiac tissue are due to this unique anisotropy.[52] In one study, Zong and colleagues showed that primary CMs cultured on an aligned electrospun poly(L-lactide) (PLLA) nanofibrous scaffold formed a mature contractile machinery (sarcomeres) indicating the importance of fiber alignment.[53] Another shortcoming of the traditional electrospinning methods is that the scaffolds are mainly two-dimensional (2D) structures composed of densely packed layers of nanofibers with limited porosity. This constraint may limit their applications in tissue engineering in which cell infiltration is required for the formation of 3D tissue constructs. Thus, it is important to develop new techniques for producing electrospun scaffolds with a robust 3D nanofibrous structure containing interconnected pores.[54]

In conclusion, 3D aligned nanofibrous scaffolds can be used as a promising tissue regeneration strategy. In comparison to 2D scaffolds, 3D aligned nanofibrous scaffolds provide additional dimension to control various cell behavior including migration, morphogenesis, and cell-cell interactions, which are important in regulating stem cell destiny and cardiac tissue regeneration.[55] With the ultimate goal of commercialization, and clinical implantation of cardiac patches, the adaptability, scalability, repeatability, and consistency of electrospinning technology undoubtedly pave the way for its industrial use and regulatory authorities.[56]

3.1.2. Engineering cardiac patches using 3D printing

3D printing of cardiac patches involves computer-controlled layer-by-layer placement of synthetic or natural polymers and cardiac cells to control the microstructures of scaffolds.[57] The 3D printing process of cardiac muscle integrates the placement of CMs with specific spatial orientation, microcirculation, and electrical conductivity elements during the assembly of the bio-fabricated heart tissue.[38] This technique enables the construction of complex porous

networks that allow for efficient nutrient delivery and uniform cell distribution across the engineered patch. 3D printing processes have been used with various materials combined with different cardiovascular cells as bioinks.[58]

The existing bioinks, which are typically made of polymers are inefficient conductors for improving electrical binding between adjacent cardiac cells. Electrically conductive nanomaterials, including graphene oxide (GO), CNTs, and AuNPs have been shown to promote CMs maturation and organization in the 3D cardiac tissue structures. Therefore, these materials can be incorporated into bioinks to print and generate 3D functional cardiac tissue constructs.[59] To print 3D structures of cardiac tissue with enhanced conductivity, Zhu *et al.* developed a GelMA-based bioink, comprising of an electrically conductive nanocomponent.[59] They incorporated GelMA-coated GNRs (G-GNRs) into GelMA/alginate(Alg) prepolymer solutions containing CMs and CFs (Figure 3A(i)), and used an air printing technique to form multiple layered constructs. As shown in Figure 3A(ii), the printability of the bioinks was evaluated while using different concentrations of Alg and calcium chloride ($CaCl_2$). In addition, the *in vitro* results showed that the encapsulated cells within the printed matrices containing G-GNRs could spread within 5 days and an interconnected and uniform layer of cells were formed after 7 days. The *in vitro* results also showed high cell viability, above 70%, when printing speeds of 5 and 10 μL/min were used (Figure 3A(iii)); however, cell viability decreased at higher speeds due to the high applied shear stresses during the printing process. Moreover, the presence of a conductive nanocomponent in their bioink improved the electrical propagation between adjacent CMs, as compared to the printed structures without G-GNRs, evidenced by enhanced expression of the gap junction protein Cx43 and higher synchronized contraction of the printed construct after two weeks. In their study, they also measured the viscosity of the G-GNR nanocomposite bioink (Figure 3A(iv)) and found that due to the presence of G-GNRs, flow consistency index increased, and flow behavior index decreased. This resulted in an amplified shear-thinning effect that could improve the printability. In another study, Basara and co-workers fabricated cardiac constructs by printing conductive titanium carbide ($Ti_3C_2T_x$) MXene in a pre-designed pattern on polyethylene glycol (PEG) hydrogels using an aerosol jet printing (Figure 3B(i)). The *in vitro* biocompatibility of the engineered constructs was confirmed by seeding human induced pluripotent stem cell derived CMs (hiPSC-derived CMs) on these patches for 7 days, which showed cell viability above 85% (Figure 3B(ii)). Moreover, their results confirmed the vital role of 3D printed $Ti_3C_2T_x$ MXene on aligning hiPSC-derived CMs with a significant increase in beta myosin heavy chain 7 (MYH7), sarco/endo plasmic reticulum calcium ATPase 2 (SERCA2), and cardiac troponin T type 2 (TNNT2) expressions (Figure 3B(iii)).[37]

Despite the high potential of 3D bioprinting, there are several limitations to the present bioinks and printing processes. For example, most of the naturally derived bioinks lack structural stability and immediately deform upon exiting the nozzle, making the printing process complicated. To address this limitation, our team utilized a freeform reversible embedding of suspended hydrogels (FRESH) printing technique to 3D print vascularized cardiac structures using soft and elastic bioinks. The printed cell-laden constructs demonstrated endothelium barrier function and spontaneous beating of cardiac muscle cells, as an important functions of cardiac tissue *in vivo*.[60] In another study, Lee and co-

workers used FRESH 3D printing method to engineer components of the human heart. They found that the printed constructs accurately reproduce patient-specific anatomical structures. These 3D printed constructs showed endothelium barrier function as well as spontaneous beating of CMs. Moreover, cardiac ventricles printed with human CMs showed directional action potential propagation, and synchronized contractions. Furthermore, when implanted subcutaneously in rats, the printed constructs evoked minimal inflammatory responses.[61]

In conclusion, 3D printed cardiac patches can provide CMs with a support matrix, allowing them to adhere and proliferate in infarcted heart tissues, as well as improve tissue regeneration by promoting angiogenesis and reducing scar formation in the defect area.[62] Future works on engineering 3D printed cardiac patches should focus on further evaluation of biocompatible bioinks and pattern design at higher resolution.

3.2. Injectable hydrogels

The use of injectable biomaterials has shown promise as an alternative treatment option following MI to preserve cardiac function.[63] These injectable materials can be administered individually or in combination with cells or growth factors to improve the mechanical and functional properties of the infarcted region. Injectable hydrogels based on various biopolymers such as GelMA,[63a] thiol-modified hyaluronic acid (HA-SH),[19e] Alg,[64] Col,[65] and fibrin[66] have been extensively studied for heart tissue regeneration. Table 2 summarizes various electroconductive injectable hydrogels applied for cardiac tissue engineering. These electroconductive injectable biomaterials not only provide structural support to the injured myocardium, but also electrically bridge the scar barrier between the healthy cardiac tissue and the viable CMs inside the scar to improve heart function.[67]

A plethora of studies has focused on designing adhesive and injectable hydrogels which could strongly attach to the myocardium, avoiding surgical suture. For example, Wu and co-workers proposed a combined therapy for MI repair, by first injecting a hydrogel into the infarcted myocardium followed by painting an adhesive hydrogel onto the outermost surface (Figure 4A(i)). The injectable hydrogel was formed using a Schiff base reaction between oxidized sodium hyaluronic acid (HA-CHO) and hydrazided hyaluronic acid (HHA), and the adhesive hydrogel was synthesized using Fe^{3+}-induced ionic coordination between dopamine-gelatin (GelDA) and dopamine functionalized polypyrrole (DA-PPy).[68] The GelDA/DA-PPy hydrogel revealed strong adhesive strength to the porcine myocardium and porcine skin (10 and 18 kPa, respectively) due to the non-covalent binding ability of the catechol moieties to the wet tissues. Additionally, the catechol-Fe^{3+} and catechol-gelatin carboxyl coordination complexation provided improved cohesion and interface adhesion. Also, the gelation behavior was investigated using an inverted vial method. As presented in Figure 4A(ii), the gelation time decreased by increasing the DA–PPy content, due to the formation of several crosslinking points. Moreover, they showed that incorporation of PPy in the hydrogel matrix provided 2.85×10^{-2} S/m electrical conductivity, which was close to that of the native myocardial tissue ($\sim 10^{-2}$ S/m). The viscoelasticity of the hydrogels was also evaluated by rheology tests (Figure 4A(iii)). It was shown that the storage moduli (G′) of the hydrogels were dominant over the loss moduli (G″), and by increasing DA–PPy, the moduli of the hydrogels were increased due to the formation of a more compact network.

Among the injectable biomaterials, thermally sensitive (thermoresponsive) hydrogels are appealing since upon injection in the body, the viscosity of the hydrogel increases, holding the material at the injection site.[69] Different synthetic and naturally derived hydrogels have been used as building blocks of thermoresponsive hydrogels for heart tissue regeneration. For example, Baei and colleagues developed a thermosensitive conductive hydrogel by using CS and AuNPs (Figure 4B(i)).[70] The addition of β-glycerophosphate disodium salt solution (β-GP) allowed the formation of homogeneous CS hydrogel within 30 min when the temperature was increased from 23 °C to 37 °C (Figure 4B(ii)), with improved organoleptic properties.[70–71] Here, the electrostatic interactions between CS, the polyol salt, and β-GP, as well as hydrogen bonding and hydrophobic interactions between CS chains induced thermoresponsive gelation behavior in CS. They evaluated the gelation time of the hydrogels based on the changes in fluidity of the solutions at 37 °C. As shown in Figure 4B(iii), the CS solution had the lowest gelation time, which was increased considerably by increasing AuNPs. Moreover, a four-point probe conductivity test showed that while the CS hydrogels were not electroconductive, increasing AuNPs concentration increased the electrical conductivities (Figure 4B(iv)). In addition, the *in vitro* studies exhibited that these hybrid hydrogels promoted the growth and viability of mesenchymal stem cells (MSCs).[70]

Another type of injectable, thermo-responsive, and conductive hydrogel was fabricated based on modified MWCNTs functionalized with carbodihydrazide (CDH) residues, which was mixed with pericardial matrix from the sheep heart.[72] To form this hydrogel, a powdered sheep-derived ECM was digested with pepsin in hydrochloric acid (HCl) to obtain a viscous solution with thermoresponsive properties, which could form a hydrogel within 10 to 20 min when the temperature was changed from 24 °C to 37 °C. *In vitro* results demonstrated that the engineered materials improved the proliferation and expression of Cx43 in CMs cultured in these hydrogels.[72]

Slow gelation can result in rapid dispersion of injected material prior to solidification, leading to cargo loss. In addition, if gelation occurs too quickly, it can clog the syringe needle before hydrogel deposition.[73] To overcome limitations of the *in situ* crosslinking of injectable hydrogels, materials with shear-thinning properties have been developed. Shear-thinning hydrogels can be injected through a syringe upon application of shear (e.g. using angled syringe needles[73]) and then reform rapidly within seconds (self-healing) when shear forces are removed. As an example, Gaffey et al. developed an injectable shear-thinning HA hydrogel seeded with endothelial progenitor cells (EPCs) to enhance cell engraftment and improve ischemic myocardium.[74] Their designed shear-thinning hydrogel assembled due to interactions of adamantine, and β-cyclodextrin modified HA. They were able to address adverse remodeling after MI, by delivering cells directly to the ischemic myocardial border zone using a syringe.

Although small and large animal studies have shown considerable improvement in critical parameters such as wall thickness, vascularization of the ischemic zone, left ventricular volumes, and cardiac function due to the application of injectable hydrogels, several critical problems associated with these biomaterials must be solved in order to develop optimum therapeutics for MI and heart failure. This includes improving material characteristics,

injection procedures, and understanding the mechanisms of action. Overall, the use of injectable biomaterials has the potential to evolve into innovative therapeutics for MI, possibly benefiting the lives of millions.[63d]

4. Conductive platforms used for therapeutic delivery in cardiac tissue engineering

Cardiac tissue regeneration strategies are frequently supplemented with cellular, pharmacological or therapeutic agents, including cardiovascular cells, stem cells, small molecules, growth factors, deoxyribonucleic acid/ ribonucleic acid (DNA/RNA), and other therapeutics to further promote cardiac tissue healing. However, controlled release of these therapeutic agents is the main challenge. One strategy to provide controlled and sustained drug delivery is to use electrical stimulation through electroconductive materials. These materials respond to changes in the electrical field, altering charge distribution, and consequently polymer conformation.[75] Moreover, the modulation of the electrical stimulus can be used to accomplish various release profiles, including burst release and slow-elution, due to the electrophoretic and electroosmotic effects.[76] Table 3 summarizes recent electroconductive platforms applied for the delivery of different therapeutic agents for cardiac tissue engineering. These constructs have been developed in various shapes, including NPs, electrospun fibrous matrices, microneedle (MN) patches, polymeric films, and injectable hydrogels.

One of the challenges after MI is the increased level of localized inflammation caused by M1 macrophages in the cardiac infarction region, intensifying adverse remodeling after MI.[77] Consequently, the regulation of inflammation via immunomodulation strategies to promote M1 polarization toward M2 macrophages was proposed by some recent studies.[78] For example, adjusting reactive oxygen species (ROS) production, which resulted in M1 differentiation to M2 macrophage phenotypes, has been proposed as a new therapeutic approach.[79] GO was introduced as an antioxidant that could decrease inflammation and inflammatory polarization of macrophages via a reduction in intracellular ROS creation. In addition, GO has been applied as a carrier for various types of genes and drugs. [63a, 80] In one study, Han *et al.* developed interleukin-4 plasmid DNA (IL-4 pDNA) loaded GO nanosheets to propagate M2 macrophages.[81] Their results revealed that IL-4 pDNA loaded GO complex decreased ROS in immune-stimulated macrophages. In addition, DNA-functionalized GO polarized M1 to M2 macrophages and promoted the cardiac repair-favorable cytokines secretion.

A common drug used in conjunction with biomaterials to enhance myocardial regeneration is 3i-1000 which is a small molecule inhibitor of GATA4-NKX2–5 transcriptional synergy, hindering CMs hypertrophic reactions and boosting myocardial regeneration. [82] Zanjanizadeh Ezazi *et al.* developed a smart electroconductive patch based on elastomeric poly(glycerol sebacate) (PGS) matrix, combined with Col type I and PPy to deliver 3i-1000.[83] To incorporate 3i-1000 drugs into the electroconductive patches, (3-aminopropyl)triethoxysilane-functionalized thermally carbonized porous silicon (APTES-TCPSi) NPs encapsulating 3i-1000 were attached to the surface of the patches. These

electroconductive patches exhibited shape customizability, high blood wettability, and controlled drug release, and could be easily implanted on the surface of the infarcted heart muscle.[83] In another study, delivery of two therapeutics, 3i-1000 and curcumin, was used to control inflammatory responses and promote cardiac regeneration.[84] The presence of curcumin provided both antioxidant and anti-inflammatory activities,[85] and the 3i-1000 showed an effective role in stimulating myocardial repair after MI infarction.[86] For example, a multifunctional patch made of nanocellulose incorporated PGS-PPy was use for the controlled release of 3i-1000 and curcumin while providing appropriate electrical conductivity and mechanical robustness similar to the native cardiac tissue.[84] The drugs were loaded either in the PGS-PPy precursor suspension and used as bioink for 3D extrusion or by direct immersion of the ready-made patches in the drug solution. The slow degradation of 3D printed PGS-based patch could prohibit initial burst release confirming its suitability for long-term therapy. These 3D printed cardiac patches demonstrated biocompatibility, controlled degradation rate, mechanical robustness, and flexibility, as well as electrical conductivity for engineering functional cardiac tissue constructs.[84]

Hydrogels can also be used for programmable drug release by accurately controlled electrostimulation. In other words, the porous morphology and high-water content of hydrogels offer exceptional capacity for loading bioactive molecules, drugs, and cells. However, intrinsic electroactive hydrogels including HA, Alg, and CS reveal weak electrical responsiveness and poor mechanical properties, limiting their application for implantable and long-term drug delivery.[87] To promote the electrical performance of hydrogels, a conductive injectable hydrogel was designed to encapsulate adipose-derived stem cells (ADSCs), lipofectamine (Lipo), and plasmid DNA-endothelial nitric oxide synthase (eNOs) nanocomplexes (Figure 5A(i)).[88] The hydrogel was developed via an *in situ* Michael addition reaction between multi-armed conductive crosslinker tetraaniline-poly(ethylene glycol) diacrylate (TA-PEGDA) and thiol modified hyaluronic acid (HA-SH). The optimized formulation of the engineered conductive hydrogel with appropriate conductivity and anti-fatigue performance was applied for treating rats after experimental MI. In this study, eNOs expression was measured *in vitro* and *in vivo* to verify the gene transfection. As demonstrated in Figure 5A(ii), TA-PEG/HA-SH/ADSCs/Gene group showed a sustained NOx expression behavior with an increased amount over 28 days. However, the NOx concentration in the MI kept a much lower level than that of normal myocardium, which was verified by the same trend in the expression of eNOs measured by quantitative reverse transcription-polymerase chain reaction (qRT-PCR) (Figure 5A(iii)). Moreover, this conductive hydrogel supported ADSCs against severe microenvironment while effectively delivering them to the infarcted area. The encapsulated plasmid DNA-eNOs nanocomplexes intensified NO in the infarcted area, which was vital for promoting neovascularization and myocardium regeneration. Consequently, a significant increase in ejection fraction (EF), shortened QRS interval, smaller infarction size, less fibrosis area, and superior vessel density were reported, confirming cardiac tissue regeneration.[88] In another study, a conductive bioadhesive hydrogel was developed for the controlled release of hydrogen sulfide (H_2S). [89] H_2S molecules can quickly diffuse across cell membranes to provide intercellular signaling without any degradation.[90] H_2S has shown various anti-inflammatory roles, mitochondrial function conservation, vasodilation, and protection against oxidative stress

in cardiovascular systems.[91] Nevertheless, therapeutic potential of H_2S was restricted due to its inherent limitations including poor water solubility and high toxicity.[92] In this study, H_2S was created by grafting 2-aminopyridine-5-thiocarboxamide (APTC) on oxidized Alg (Alg-CHO) to control the release of H_2S without inducing toxicity (Figure 5B(i)).[89] To provide electrical impulse signals between myocardial cells, Alg-CHO-APTC was grafted to tetraaniline (TA) leading to the formation of a multifunctional copolymer ALG−TA−APTC. Herein, the hydrogels with conductivity and controllable H_2S-releasing ability were developed via the Schiff-base reaction between the aldehyde groups of ALG−TA−APTC and amine groups of gelatin. As shown in Figure 5B(ii), a sustained and controllable release of H_2S was achieved *in vitro* for the ALG-CHO/ALG−TA−APTC/ Gelatin hydrogel group. In this study, the methylene blue method was utilized for the detection of the total sulfide concentration to illustrate the H_2S concentration in the myocardium. Figure 5B(iii) shows that the concentration of sulfide in a normal myocardium was detected as 0.16 μmol/g, while after MI, the sulfide decreased to a relatively low level of 0.12 μmol/g. Furthermore, the therapeutic effect of the adipose-derived stem cells (ADSCs) loaded hydrogel on acute MI was investigated and results demonstrated the long-stability and integration with myocardial tissues. In addition, while electrical conductivity of the hydrogel enhanced the electrical pulse conduction between myocardial cells, H_2S promoted neovascularization and anti-inflammatory effects in the MI area.[89]

The development of nanocomposite hydrogels is another strategy to improve both the mechanical performance and electroconductive properties of electrically controlled drug release platforms.[76] In one study, a nanocomposite conductive and injectable hydrogel with effective release of vascular endothelial growth factor-165 ($VEGF_{165}$) pro-angiogenic gene was developed for MI therapy.[63a] The pro-angiogenic gene was loaded in GO (fGO_{VEGF}) and consequently encapsulated in a low-modulus GelMA hydrogel. After injection of fGO_{VEGF}/GelMA to the infarcted heart, a substantial improvement in microcapillary density at the infused peri-infarct region and a decrease in scar formation were observed.[63a] In addition, compared to control group (pure GelMA), improvement in cardiac function, based on echocardiography (after the fGO_{VEGF}/GelMA injection) was reported. This nonviral hybrid complex of fGO and DNA was introduced as a promising strategy for MI therapy. [63a] In another study, to develop an electroconductive hydrogel for controlled release of dexamethasone, polyacrylamide (PAM)/ CS interpenetrating polymeric network (IPN) was applied as the hydrogel matrix where PPy nanorods were formed *in situ* inside this hydrogel network.[93] According to Figure 5C(i), during the polymerization process, dexamethasone was added to the prepolymer solution to provide electrostatic interactions with the PPy. As shown in Figure 5C(ii), while the tough PAM/CS IPN matrix revealed an unstimulated burst release of dexamethasone, incorporation of PPy provided a controlled release of dexamethasone using external electrical stimulation. The cumulative release was also improved by increasing the PPy concentration and stimulation voltage. It was mentioned that during the oxidative polymerization process, the free anionic drug was incorporated in the PPy matrix as a dopant molecule. When the PPy was electrochemically reduced under negative potentials, the anionic drug was released because the positive charge state of the polymer backbone was changed (Figure 5C(iii)). This electrical stimulation could also

promote the elongation and activity of C2C12 cultured on this electroconductive hydrogel. [93]

Recently, MN array patches have been also applied for the controlled release of drugs for cardiac disease therapy. In this regard, a CNTs integrated MN patch was developed as an innovative strategy for treating cardiac diseases.[94] This patch could accommodate hiPSC-derived CM attachment and alignment for the treatment of MI using a mouse model. As shown in Figure 5D(i), this multi-layer patch had a bottom layer encapsulating angiogenic and antiphlogistic drug, a middle layer made of parallel aligned CNTs, and an upper layer of GelMA hydrogel. This electroconductive MN patch with an anisotropic structure could induce cell alignment (Figure 5D(ii)) and provide a platform for electrical signal conduction among cells. In addition, the aligned CNT layer could ensure the simultaneous contraction of CMs cultured on the patch (Figure 5D(iii)). Moreover, VEGF and interleukin-10 (IL-10) loaded bottom layer of MN patch could facilitate revascularization and hinder inflammatory reaction of the damaged zone, respectively.

In conclusion, three factors are necessary for a successful design of heart-targeted drug delivery systems. First, it is important to learn the basics of different cardiac disorders, such as their origin, pathological manifestations, clinical aspects, and desired therapy. Second, appropriate heart-targeted drug carriers must be chosen, and their active targeting characteristics should be adjusted in order to increase the stability of loaded therapeutics. Finally, the right targeting ligands should be identified to guarantee that the nanocarriers connect specifically with complimentary molecules on the surface of the targeted cells.[95]

5. Conclusions

Cardiac tissue engineering has been developed as a possible alternative to improve heart function in patients with heart failure. In this regard, promoting electrical integration of cardiac scaffolds with the host tissue may help restore the functionality of the injured heart. There are several forms of electroconductive materials employed in cardiac tissue engineering, including gold and carbon-based nanomaterials, as well as electroactive polymers (e.g., PANI and PPy). The engineered scaffolds containing conductive agents have been developed using a variety of methods, most notably 3D printing and electrospinning. These electroconductive scaffolds encapsulated with CMs and/or therapeutic agents (e.g., small molecule drugs, growth factors, and RNA-based therapeutics) have shown to promote cardiac tissue regeneration through CMs stimulation and controlled release of different bioactive molecules. It is worth noting that, while a plethora of studies summarized in this paper aimed at cardiovascular disease therapy using electroconductive materials, none of them satisfy all the needs for successful *in vivo* applications, and we are still waiting for an appropriate cure to reach patients. Therefore, the design and implementation of preclinical trials that can simulate native tissue microenvironment will help to reach clinical trials. In this regard, clinically relevant and meticulously designed pre-clinical trials, especially large animal studies, are required to expedite the translation of these findings.[73] However, since genetic and environmental variables play a prominent role in cardiovascular diseases, matching a specific condition to a single experimental model is challenging. As a result, no model precisely replicates the complication of human body. To put in a nutshell, cost,

equipment, and the need for specialist employees should all be taken into account and the models that best imitate the condition should be chosen based on all of these factors and the available budgets.[96]

Despite all the existing obstacles, the area of injectable/printable biomaterial-based regenerative medicine for cardiovascular disease has great potential to benefit a large number of patients, and it is expected that these strategies would quickly progress through clinical trials.

Acknowledgements

Biographies

Mahsa Ghovvati is currently a postdoctoral researcher at the University of California-Los Angeles (UCLA) with expertise in hydrogel synthesis and characterization, cell culture, *in vivo* studies and also modeling and simulation of bioprocesses. Her research is mainly focused on designing and developing bio-adhesives for various biomedical applications, including but not limited to surgical sealants to better utilize their therapeutic potential in order to address medical challenges and improve patients' health-related quality of life.

Nasim Annabi is an Assistant Professor in the Department of Chemical and Biomolecular Engineering at University of California, Los Angeles (UCLA). Her multidisciplinary research program at UCLA aims to integrate novel chemistries with microscale technologies to develop the next generation of biomaterials for medical applications. In addition, her group has devised innovative strategies for the development of surgical sealants for the repair and sealing of elastic tissues. Her interdisciplinary research has been recognized by several awards such as the 2020 NSEF Young Investigator Award of American Institute of Chemical Engineers (AIChE), the 2021 Young Investigator Award from the Society for Biomaterials (SFB), and the 2021 Biomaterials Science Lectureship Award from the Royal Society of Chemistry (RSC).

Reza Ardehali is a physician-scientist studying the molecular mechanisms in heart development and disease. Specifically, his lab is interested in the intrinsic signaling that trigger cardiac regeneration and molecular events that instruct cardiac progenitors to adopt a specific cell fate during development. He is also a practicing cardiologist with subspecialty in Advanced Heart Failure and Transplantation. He is currently the Associate Chief of Cardiology, Regenerative Medicine at David Geffen UCLA School of Medicine.

References:

[1]. Mc Namara K, Alzubaidi H, Jackson JK, Integrated pharmacy research & practice 2019, 8, 1. [PubMed: 30788283]

[2]. Agarwal T, Fortunato GM, Hann SY, Ayan B, Vajanthri KY, Presutti D, Cui H, Chan AHP, Costantini M, Onesto V, Di Natale C, Materials Science and Engineering: C 2021, 112057. [PubMed: 33947551]

[3]. Small EM, Thatcher JE, Sutherland LB, Kinoshita H, Gerard RD, Richardson JA, DiMaio JM, Sadek H, Kuwahara K, Olson EN, Circulation research 2010, 107, 294. [PubMed: 20558820]

[4]. Kittleson MM, Kobashigawa JA, JACC: Heart Failure 2017, 5, 857. [PubMed: 29191293]

[5]. Shadrin IY, Allen BW, Qian Y, Jackman CP, Carlson AL, Juhas ME, Bursac N, Nature communications 2017, 8, 1.

[6]. Duan B, Annals of biomedical engineering 2017, 45, 195. [PubMed: 27066785]

[7]. John M, Bailey LL, Annals of cardiothoracic surgery 2018, 7, 118. [PubMed: 29492389]

[8]. Sepantafar M, Maheronnaghsh R, Mohammadi H, Rajabi-Zeleti S, Annabi N, Aghdami N, Baharvand H, Biotechnology advances 2016, 34, 362. [PubMed: 26976812]

[9]. Joggerst SJ, Hatzopoulos AK, Expert reviews in molecular medicine 2009, 11.

[10]. a)Nguyen AH, Marsh P, Schmiess-Heine L, Burke PJ, Lee A, Lee J, Cao H, Journal of biological engineering 2019, 13, 1; [PubMed: 30627214] b)Monteiro LM, Vasques-Nóvoa F, Ferreira L, Nascimento DS, NPJ Regenerative medicine 2017, 2, 1. [PubMed: 29302338]

[11]. Majid QA, Fricker AT, Gregory DA, Davidenko N, Hernandez Cruz O, Jabbour RJ, Owen TJ, Basnett P, Lukasiewicz B, Stevens M, Best S, Frontiers in cardiovascular medicine 2020, 7, 192.

[12]. a)Ghovvati M, Baghdasarian S, Baidya A, Dhal J, Annabi N, Journal of Biomedical Materials Research Part B: Applied Biomaterials 2022, n/a;b)Baghdasarian S, Saleh B, Baidya A, Kim H, Ghovvati M, Sani ES, Haghniaz R, Madhu S, Kanelli M, Noshadi I, Annabi N, Materials Today Bio 2022, 13, 100199.

[13]. a)Mousavi A, Vahdat S, Baheiraei N, Razavi M, Norahan MH, Baharvand H, ACS Biomaterials Science & Engineering 2020;b)Burnstine-Townley A, Eshel Y, Amdursky N, Advanced Functional Materials 2020, 30, 1901369.

[14]. a)Li H, Bao M, Nie Y, Heart failure reviews 2020, 1;b)Xu Y, Guan J, Bioactive materials 2016, 1, 18; [PubMed: 29744392] c)Mostafavi A, Samandari M, Karvar M, Ghovvati M, Endo Y, Sinha I, Annabi N, Tamayol A, Applied Physics Reviews 2021, 8, 041415. [PubMed: 34970378]

[15]. Camci-Unal G, Annabi N, Dokmeci MR, Liao R, Khademhosseini A, NPG Asia Materials 2014, 6, e99.

[16]. a)Wang PY, Yu J, Lin JH, Tsai WB, Acta biomaterialia 2011, 7, 3285; [PubMed: 21664306] b)Annabi N, Tsang K, Mithieux SM, Nikkhah M, Ameri A, Khademhosseini A, Weiss AS, Advanced functional materials 2013, 23, 4950.

[17]. Kharaziha M, Nikkhah M, Shin SR, Annabi N, Masoumi N, Gaharwar AK, Camci-Unal G, Khademhosseini A, Biomaterials 2013, 34, 6355. [PubMed: 23747008]

[18]. a)Liang S, Zhang Y, Wang H, Xu Z, Chen J, Bao R, Tan B, Cui Y, Fan G, Wang W, Wang W, Liu W, Advanced Materials 2018, 30, 1704235;b)Li Y, Wei L, Lan L, Gao Y, Zhang Q, Dawit H, Mao J, Guo L, Shen L, Wang L, Acta Biomaterialia 2021.

[19]. a)Dong R, Ma PX, Guo B, Biomaterials 2020, 229, 119584; [PubMed: 31704468] b)Solazzo M, O'Brien FJ, Nicolosi V, Monaghan MG, APL bioengineering 2019, 3, 041501; [PubMed: 31650097] c)Kharaziha M, Memic A, Akbari M, Brafman DA, Nikkhah M, Advanced healthcare materials 2016, 5, 1533; [PubMed: 27199266] d)Eom T, Woo K, Shim BS, Applied Chemistry for Engineering 2016, 27, 115;e)Bao R, Tan B, Liang S, Zhang N, Wang W, Liu W, Biomaterials 2017, 122, 63; [PubMed: 28107665] f)Golafshan N, Kharaziha M, Fathi M, Carbon 2017, 111, 752.

[20]. Zhou J, Vijayavenkataraman S, Bioprinting 2021, 24, e00166.

[21]. a)Alkilany AM, Murphy CJ, J Nanopart Res 2010, 12, 2313; [PubMed: 21170131] b)Ray PC, Yu H, Fu PP, J Environ Sci Health C Environ Carcinog Ecotoxicol Rev 2009, 27, 1; [PubMed: 19204862] c)Li X, Wang L, Fan Y, Feng Q, Cui F.-z., Journal of Nanomaterials 2012, 2012, 548389.

[22]. Safe handling and use of carbon nanotubes, https://www.safeworkaustralia.gov.au/, accessed.

[23]. a)Vashist A, Kaushik A, Vashist A, Sagar V, Ghosal A, Gupta YK, Ahmad S, Nair M, Advanced healthcare materials 2018, 7, 1701213;b)Pok S, Vitale F, Eichmann SL, Benavides OM, Pasquali M, Jacot JG, ACS nano 2014, 8, 9822. [PubMed: 25233037]

[24]. Thoniyot P, Tan MJ, Karim AA, Young DJ, Loh XJ, Advanced Science 2015, 2, 1400010. [PubMed: 27980900]

[25]. Baei P, Hosseini M, Baharvand H, Pahlavan S, Journal of Biomedical Materials Research Part A 2020, 108, 1203. [PubMed: 32034936]

[26]. a)Gorain B, Choudhury H, Pandey M, Kesharwani P, Abeer MM, Tekade RK, Hussain Z, Biomedicine & Pharmacotherapy 2018, 104, 496; [PubMed: 29800914] b)Balint R, Cassidy NJ, Cartmell SH, Acta biomaterialia 2014, 10, 2341; [PubMed: 24556448] c)Yadid M, Feiner R, Dvir T, Nano letters 2019, 19, 2198; [PubMed: 30884238] d)Nulwala H, Mirjafari A, Zhou X, European Polymer Journal 2018, 108, 390;e)Cha C, Shin SR, Annabi N, Dokmeci MR, Khademhosseini A, ACS nano 2013, 7, 2891; [PubMed: 23560817] f)Shin SR, Li YC, Jang HL, Khoshakhlagh P, Akbari M, Nasajpour A, Zhang YS, Tamayol A, Khademhosseini A, Advanced drug delivery reviews 2016, 105, 255. [PubMed: 27037064]

[27]. a)Kharaziha M, Shin SR, Nikkhah M, Topkaya SN, Masoumi N, Annabi N, Dokmeci MR, Khademhosseini A, Biomaterials 2014, 35, 7346; [PubMed: 24927679] b)Spencer AR, Shirzaei Sani E, Soucy JR, Corbet CC, Primbetova A, Koppes RA, Annabi N, ACS applied materials & interfaces 2019, 11, 30518; [PubMed: 31373791] c)Noshadi I, Walker BW, Portillo-Lara R, Sani ES, Gomes N, Aziziyan MR, Annabi N, Scientific reports 2017, 7, 1. [PubMed: 28127051]

[28]. a)Burnstine-Townley A, Eshel Y, Amdursky N, Advanced Functional Materials 2020, 30, 1901369;b)Ashtari K, Nazari H, Ko H, Tebon P, Akhshik M, Akbari M, Alhosseini SN, Mozafari M, Mehravi B, Soleimani M, Ardehali R, Advanced Drug Delivery Reviews 2019, 144, 162. [PubMed: 31176755]

[29]. Esmaeili H, Patino-Guerrero A, Hasany M, Ansari MO, Memic A, Dolatshahi-Pirouz A, Nikkhah M, Acta Biomaterialia 2022, 139, 118. [PubMed: 34455109]

[30]. Hendrickson T, Mancino C, Whitney L, Tsao C, Rahimi M, Taraballi F, Nanomedicine: Nanotechnology, Biology and Medicine 2021, 33, 102367. [PubMed: 33549819]

[31]. Souders CA, Bowers SL, Baudino TA, Circulation research 2009, 105, 1164. [PubMed: 19959782]

[32]. Sanchis-Gomar F, Perez-Quilis C, Leischik R, Lucia A, Annals of translational medicine 2016, 4.

[33]. Mohan RA, Boukens BJ, Christoffels VM, Pediatric cardiology 2018, 39, 1107. [PubMed: 29774393]

[34]. Grant AO, Circulation: Arrhythmia and Electrophysiology 2009, 2, 185. [PubMed: 19808464]

[35]. a)Cutler MJ, Jeyaraj D, Rosenbaum DS, Trends in pharmacological sciences 2011, 32, 174; [PubMed: 21316769] b)Kistamás K, Veress R, Horvath B, Banyasz T, Nánási PP, Eisner DA, Frontiers in pharmacology 2020, 11, 72. [PubMed: 32161540]

[36]. Lister Z, Rayner KJ, Suuronen EJ, Frontiers in bioengineering and biotechnology 2016, 4, 62. [PubMed: 27486578]

[37]. Basara G, Saeidi-Javash M, Ren X, Bahcecioglu G, Wyatt BC, Anasori B, Zhang Y, Zorlutuna P, Acta biomaterialia 2020, DOI: 10.1016/j.actbio.2020.12.033.

[38]. Birla RK, Williams SK, APL Bioeng 2020, 4, 010903. [PubMed: 32095736]

[39]. Pedrotty DM, Kuzmenko V, Karabulut E, Sugrue AM, Livia C, Vaidya VR, McLeod CJ, Asirvatham SJ, Gatenholm P, Kapa S, Circulation: Arrhythmia and Electrophysiology 2019, 12, e006920. [PubMed: 30845835]

[40]. Nguyen AH, Marsh P, Schmiess-Heine L, Burke PJ, Lee A, Lee J, Cao H, Journal of Biological Engineering 2019, 13, 57. [PubMed: 31297148]

[41]. a)Bray M-A, Sheehy SP, Parker KK, Cell Motility 2008, 65, 641;b)Feinberg AW, Alford PW, Jin H, Ripplinger CM, Werdich AA, Sheehy SP, Grosberg A, Parker KK, Biomaterials 2012, 33, 5732; [PubMed: 22594976] c)Chung C.-y., Bien H, Sobie EA, Dasari V, McKinnon D, Rosati B, Entcheva E, The FASEB Journal 2011, 25, 851; [PubMed: 21084696] d)Geisse NA, Sheehy SP, Parker KK, In Vitro Cellular & Developmental Biology - Animal 2009, 45, 343. [PubMed: 19252956]

[42]. a)Smith AST, Yoo H, Yi H, Ahn EH, Lee JH, Shao G, Nagornyak E, Laflamme MA, Murry CE, Kim D-H, Chem Commun (Camb) 2017, 53, 7412; [PubMed: 28634611] b)Hu T, Wu Y, Zhao X, Wang L, Bi L, Ma PX, Guo B, Chemical Engineering Journal 2019, 366, 208;c)Tsui JH, Ostrovsky-Snider NA, Yama DMP, Donohue JD, Choi JS, Chavanachat R, Larson JD, Murphy AR, Kim D-H, Journal of Materials Chemistry B 2018, 6, 7185. [PubMed: 31448124]

[43]. a)Walker BW, Lara RP, Yu CH, Sani ES, Kimball W, Joyce S, Annabi N, Biomaterials 2019, 207, 89; [PubMed: 30965152] b)Huyer LD, Montgomery M, Zhao Y, Xiao Y, Conant G, Korolj A, Radisic M, Biomedical Materials 2015, 10, 034004. [PubMed: 25989939]

[44]. Olvera D, Sohrabi Molina M, Hendy G, Monaghan MG, Advanced Functional Materials 2020, 30, 1909880.

[45]. Navaei A, Saini H, Christenson W, Sullivan RT, Ros R, Nikkhah M, Acta biomaterialia 2016, 41, 133. [PubMed: 27212425]

[46]. Kapnisi M, Mansfield C, Marijon C, Guex AG, Perbellini F, Bardi I, Humphrey EJ, Puetzer JL, Mawad D, Koutsogeorgis DC, Stuckey DJ, Terracciano CM, Harding SE, Stevens MM, Advanced functional materials 2018, 28, 1800618. [PubMed: 29875619]

[47]. a)Hosoyama K, Ahumada M, McTiernan CD, Davis DR, Variola F, Ruel M, Liang W, Suuronen EJ, Alarcon EI, ACS applied materials & interfaces 2018, 10, 44668; [PubMed: 30508481] b)Ajdary R, Ezazi NZ, Correia A, Kemell M, Huan S, Ruskoaho HJ, Hirvonen J, Santos HA, Rojas OJ, Advanced Functional Materials 2020, 30, 2003440;c)Kai D, Prabhakaran MP, Jin G, Ramakrishna S, Journal of Materials Chemistry B 2013, 1, 2305. [PubMed: 32260884]

[48]. Nun N, Cruz M, Jain T, Tseng Y-M, Menefee J, Jatana S, Patil PS, Leipzig ND, McDonald C, Maytin E, Joy A, Biomacromolecules 2020, 21, 4030. [PubMed: 32902971]

[49]. Shin M, Ishii O, Sueda T, Vacanti JP, Biomaterials 2004, 25, 3717. [PubMed: 15020147]

[50]. Kitsara M, Agbulut O, Kontziampasis D, Chen Y, Menasché P, Acta biomaterialia 2017, 48, 20. [PubMed: 27826001]

[51]. Kitsara M, Joanne P, Boitard SE, Ben Dhiab I, Poinard B, Menasché P, Gagnieu C, Forest P, Agbulut O, Chen Y, Microelectronic Engineering 2015, 144, 46.

[52]. Liu W, Thomopoulos S, Xia Y, Advanced healthcare materials 2012, 1, 10. [PubMed: 23184683]

[53]. Zong X, Bien H, Chung CY, Yin L, Fang D, Hsiao BS, Chu B, Entcheva E, Biomaterials 2005, 26, 5330. [PubMed: 15814131]

[54]. Chen Y, Shafiq M, Liu M, Morsi Y, Mo X, Bioactive Materials 2020, 5, 963. [PubMed: 32671291]

[55]. Jin G, He R, Sha B, Li W, Qing H, Teng R, Xu F, Materials science & engineering. C, Materials for biological applications 2018, 92, 995. [PubMed: 30184829]

[56]. Boffito M, Tonda-Turo C, Ciardelli G, in Electrofluidodynamic Technologies (EFDTs) for Biomaterials and Medical Devices, DOI: 10.1016/B978-0-08-101745-6.00012-8 (Eds: Guarino V, Ambrosio L), Woodhead Publishing 2018, p. 221.

[57]. Taylor DA, Hochman-Mendez C, Huelsmann J, Elgalad A, Sampaio LC, in Principles of Tissue Engineering (Fifth Edition), DOI: 10.1016/B978-0-12-818422-6.00084-8 (Eds: Lanza R, Langer R, Vacanti JP, Atala A), Academic Press 2020, p. 1521.

[58]. Streeter BW, Davis ME, Advances in experimental medicine and biology 2019, 1144, 1. [PubMed: 30542805]

[59]. Zhu K, Shin SR, van Kempen T, Li YC, Ponraj V, Nasajpour A, Mandla S, Hu N, Liu X, Leijten J, Lin YD, Hussain MA, Zhang YS, Tamayol A, Khademhosseini A, Adv Funct Mater 2017, 27.

[60]. Lee S, Sani ES, Spencer AR, Guan Y, Weiss AS, Annabi N, Advanced materials (Deerfield Beach, Fla.) 2020, 32, e2003915.

[61]. Lee A, Hudson AR, Shiwarski DJ, Tashman JW, Hinton TJ, Yerneni S, Bliley JM, Campbell PG, Feinberg AW, Science 2019, 365, 482. [PubMed: 31371612]

[62]. a)Gaebel R, Ma N, Liu J, Guan J, Koch L, Klopsch C, Gruene M, Toelk A, Wang W, Mark P, Wang F, Chichkov B, Li W, Steinhoff G, Biomaterials 2011, 32, 9218; [PubMed: 21911255] b)Yeung E, Fukunishi T, Bai Y, Bedja D, Pitaktong I, Mattson G, Jeyaram A, Lui C, Ong CS, Inoue T, Matsushita H, Abdollahi S, Jay SM, Hibino N, Journal of Tissue Engineering and Regenerative Medicine 2019, 13, 2031. [PubMed: 31408915]

[63]. a)Paul A, Hasan A, Kindi HA, Gaharwar AK, Rao VTS, Nikkhah M, Shin SR, Krafft D, Dokmeci MR, Shum-Tim D, Khademhosseini A, ACS Nano 2014, 8, 8050; [PubMed: 24988275] b)Tian H, Huang M-L, Liu K-Y, Jia Z-B, Sun L, Jiang S-L, Liu W, Kinkaid HYM, Wu J, Li R-K, Cell Transplantation 2012, 21, 1039; [PubMed: 21944319] c)Wu J, Zeng F, Huang XP, Chung JC, Konecny F, Weisel RD, Li RK, Biomaterials 2011, 32, 579; [PubMed: 20932570] d)Johnson TD, Christman KL, Expert opinion on drug delivery 2013, 10, 59. [PubMed: 23140533]

[64]. Leor J, Tuvia S, Guetta V, Manczur F, Castel D, Willenz U, Petneházy O, Landa N, Feinberg MS, Konen E, Goitein O, Tsur-Gang O, Shaul M, Klapper L, Cohen S, Journal of the American College of Cardiology 2009, 54, 1014. [PubMed: 19729119]

[65]. a)Leung BM, Miyagi Y, Li R-K, Sefton MV, Journal of tissue engineering and regenerative medicine 2015, 9, 1247; [PubMed: 23505249] b)Blackburn NJ, Sofrenovic T, Kuraitis D, Ahmadi A, McNeill B, Deng C, Rayner KJ, Zhong Z, Ruel M, Suuronen EJ, Biomaterials 2015, 39, 182. [PubMed: 25468370]

[66]. Zhang X, Wang H, Ma X, Adila A, Wang B, Liu F, Chen B, Wang C, Ma Y, Experimental biology and medicine (Maywood, N.J.) 2010, 235, 1505.

[67]. Mihic A, Cui Z, Wu J, Vlacic G, Miyagi Y, Li SH, Lu S, Sung HW, Weisel RD, Li RK, Circulation 2015, 132, 772. [PubMed: 26304669]

[68]. Wu T, Cui C, Huang Y, Liu Y, Fan C, Han X, Yang Y, Xu Z, Liu B, Fan G, Liu W, ACS applied materials & interfaces 2019, 12, 2039.

[69]. Fujimoto KL, Ma Z, Nelson DM, Hashizume R, Guan J, Tobita K, Wagner WR, Biomaterials 2009, 30, 4357. [PubMed: 19487021]

[70]. Baei P, Jalili-Firoozinezhad S, Rajabi-Zeleti S, Tafazzoli-Shadpour M, Baharvand H, Aghdami N, Materials science & engineering. C, Materials for biological applications 2016, 63, 131. [PubMed: 27040204]

[71]. Szymańska E, Sosnowska K, Miltyk W, Rusak M, Basa A, Winnicka K, Polymers 2015, 7, 2223.

[72]. Roshanbinfar K, Hilborn J, Varghese OP, Oommen OP, RSC Advances 2017, 7, 31980.

[73]. Chen MH, Wang LL, Chung JJ, Kim Y-H, Atluri P, Burdick JA, ACS Biomaterials Science & Engineering 2017, 3, 3146. [PubMed: 29250593]

[74]. Gaffey AC, Chen MH, Venkataraman CM, Trubelja A, Rodell CB, Dinh PV, Hung G, MacArthur JW, Soopan RV, Burdick JA, Atluri P, J Thorac Cardiovasc Surg 2015, 150, 1268. [PubMed: 26293548]

[75]. Qu J, Zhao X, Ma PX, Guo B, Acta biomaterialia 2018, 72, 55. [PubMed: 29555459]

[76]. Yi YT, Sun JY, Lu YW, Liao YC, Biomicrofluidics 2015, 9, 022401. [PubMed: 25825612]

[77]. Wang Z, Huang S, Sheng Y, Peng X, Liu H, Jin N, Cai J, Shu Y, Li T, Li P, Fan C, Hu X, Zhang W, Long R, You Y, Huang C, Song Y, Xiang C, Wang J, Yang Y, Liu K, Cardiovascular Research 2017, 113, 475. [PubMed: 28339742]

[78]. a)Bloise N, Rountree I, Polucha C, Montagna G, Visai L, Coulombe KLK, Munarin F, Front Bioeng Biotechnol 2020, 8, 292; [PubMed: 32318563] b)Xiong YY, Gong ZT, Tang RJ, Yang

YJ, Theranostics 2021, 11, 1046; [PubMed: 33391520] c)Qasim M, Haq F, Kang M-H, Kim J-H, in Int J Nanomedicine, Vol. 14, 2019, 1311; [PubMed: 30863063] d)Panahi M, Papanikolaou A, Torabi A, Zhang J-G, Khan H, Vazir A, Hasham MG, Cleland JGF, Rosenthal NA, Harding SE, Sattler S, Cardiovascular Research 2018, 114, 1445; [PubMed: 30010800] e)Pan W, Zhu Y, Meng X, Zhang C, Yang Y, Bei Y, J Cardiovasc Transl Res 2019, 12, 28; [PubMed: 30374796] f)Zlatanova I, Pinto C, Silvestre JS, Front Cardiovasc Med 2016, 3, 40. [PubMed: 27790620]

[79]. a)Jeong HY, Kang WS, Hong MH, Jeong HC, Shin MG, Jeong MH, Kim YS, Ahn Y, Sci Rep 2015, 5, 15768; [PubMed: 26510961] b)Kim YS, Jeong HY, Kim AR, Kim WH, Cho H, Um J, Seo Y, Kang WS, Jin SW, Kim MC, Kim YC, Jung DW, Williams DR, Ahn Y, Sci Rep 2016, 6, 30726. [PubMed: 27510556]

[80]. a)Choi HY, Lee TJ, Yang GM, Oh J, Won J, Han J, Jeong GJ, Kim J, Kim JH, Kim BS, Cho SG, J Control Release 2016, 235, 222; [PubMed: 27266364] b)Wang C, Wang X, Lu T, Liu F, Guo B, Wen N, Du Y, Lin H, Tang J, Zhang L, RSC Advances 2016, 6, 22461.

[81]. Han J, Kim YS, Lim MY, Kim HY, Kong S, Kang M, Choo YW, Jun JH, Ryu S, Jeong HY, Park J, Acs Nano 2018, 12, 1959. [PubMed: 29397689]

[82]. Kinnunen SM, Tölli M, Välimäki MJ, Gao E, Szabo Z, Rysä J, Ferreira MP, Ohukainen P, Serpi R, Correia A, Mäkilä E, Scientific reports 2018, 8, 1. [PubMed: 29311619]

[83]. Zanjanizadeh Ezazi N, Ajdary R, Correia A, Mäkilä E, Salonen J, Kemell M, Hirvonen J, Rojas OJ, Ruskoaho HJ, Santos HA, ACS applied materials & interfaces 2020, 12, 6899. [PubMed: 31967771]

[84]. Ajdary R, Ezazi NZ, Correia A, Kemell M, Huan S, Ruskoaho HJ, Hirvonen J, Santos HA, Rojas OJ, Advanced Functional Materials 2020, 30, 2003440.

[85]. Rahnavard M, Hassanpour M, Ahmadi M, Heidarzadeh M, Amini H, Javanmard MZ, Nouri M, Rahbarghazi R, Safaie N, Journal of cellular biochemistry 2019, 120, 11965.

[86]. Kinnunen SM, Tölli M, Välimäki MJ, Gao E, Szabo Z, Rysä J, Ferreira MP, Ohukainen P, Serpi R, Correia A, Mäkilä E, Scientific reports 2018, 8, 1. [PubMed: 29311619]

[87]. Emmanuel BD, Abu-Thabit NY, Ngwuluka NC, in Stimuli Responsive Polymeric Nanocarriers for Drug Delivery Applications, Volume 1, DOI: 10.1016/B978-0-08-101997-9.00014-X (Eds: Makhlouf ASH, Abu-Thabit NY), Woodhead Publishing 2018, p. 267.

[88]. Wang W, Tan B, Chen J, Bao R, Zhang X, Liang S, Shang Y, Liang W, Cui Y, Fan G, Jia H, Liu W, Biomaterials 2018, 160, 69. [PubMed: 29396380]

[89]. Liang W, Chen J, Li L, Li M, Wei X, Tan B, Shang Y, Fan G, Wang W, Liu W, ACS applied materials & interfaces 2019, 11, 14619. [PubMed: 30939870]

[90]. Predmore BL, Lefer DJ, Journal of cardiovascular translational research 2010, 3, 487. [PubMed: 20628909]

[91]. Zhang Y, Wang J, Li H, Yuan L, Wang L, Wu B, Ge J, Science China Life Sciences 2015, 58, 1126. [PubMed: 26246380]

[92]. Connal LA, Journal of Materials Chemistry B 2018, 6, 7122. [PubMed: 32254628]

[93]. Gan D, Han L, Wang M, Xing W, Xu T, Zhang H, Wang K, Fang L, Lu X, ACS applied materials & interfaces 2018, 10, 36218. [PubMed: 30251533]

[94]. Sun L, Zhu X, Zhang X, Chen G, Bian F, Wang J, Zhou Q, Wang D, Zhao Y, Chemical Engineering Journal 2021, 414, 128723.

[95]. a)Liu M, Li M, Wang G, Liu X, Liu D, Peng H, Wang Q, J Biomed Nanotechnol 2014, 10, 2038; [PubMed: 25992448] b)Ordikhani F, Zandi N, Mazaheri M, Luther GA, Ghovvati M, Akbarzadeh A, Annabi N, Medicinal Research Reviews 2021, 41, 1221. [PubMed: 33347711]

[96]. Zaragoza C, Gomez-Guerrero C, Martin-Ventura JL, Blanco-Colio L, Lavin B, Mallavia B, Tarin C, Mas S, Ortiz A, Egido J, Journal of Biomedicine and Biotechnology 2011, 2011, 497841. [PubMed: 21403831]

[97]. Mohammadi Amirabad L, Massumi M, Shamsara M, Shabani I, Amari A, Mossahebi Mohammadi M, Hosseinzadeh S, Vakilian S, Steinbach SK, Khorramizadeh MR, Soleimani M, Barzin J, ACS applied materials & interfaces 2017, 9, 6849. [PubMed: 28116894]

[98]. Hsiao CW, Bai MY, Chang Y, Chung MF, Lee TY, Wu CT, Maiti B, Liao ZX, Li RK, Sung HW, Biomaterials 2013, 34, 1063. [PubMed: 23164424]

[99]. Roshanbinfar K, Vogt L, Ruther F, Roether JA, Boccaccini AR, Engel FB, Advanced Functional Materials 2020, 30, 1908612.

[100]. Gelmi A, Cieslar-Pobuda A, de Muinck E, Los M, Rafat M, Jager EW, Advanced healthcare materials 2016, 5, 1471. [PubMed: 27126086]

[101]. Wu Y, Wang L, Guo B, Ma PX, ACS Nano 2017, 11, 5646. [PubMed: 28590127]

[102]. Liu Y, Lu J, Xu G, Wei J, Zhang Z, Li X, Materials science & engineering. C, Materials for biological applications 2016, 69, 865. [PubMed: 27612781]

[103]. Nazari H, Heirani-Tabasi A, Hajiabbas M, Khalili M, Shahsavari Alavijeh M, Hatamie S, Mahdavi Gorabi A, Esmaeili E, Ahmadi Tafti SH, Polymers for Advanced Technologies 2020, 31, 248.

[104]. Arumugam R, Srinadhu ES, Subramanian B, Nallani S, Medical Hypotheses 2019, 122, 31. [PubMed: 30593417]

[105]. Liang Y, Mitriashkin A, Lim TT, Goh JCH, Biomaterials 2021, 276, 121008. [PubMed: 34265591]

[106]. Tsui JH, Leonard A, Camp ND, Long JT, Nawas ZY, Chavanachat R, Smith AS, Choi JS, Dong Z, Ahn EH, Wolf-Yadlin A, Biomaterials 2021, 272, 120764. [PubMed: 33798964]

[107]. Norahan MH, Amroon M, Ghahremanzadeh R, Mahmoodi M, Baheiraei N, Journal of biomedical materials research. Part A 2019, 107, 204. [PubMed: 30371973]

[108]. Shin SR, Zihlmann C, Akbari M, Assawes P, Cheung L, Zhang K, Manoharan V, Zhang YS, Yüksekkaya M, Wan K-T, Nikkhah M, Dokmeci MR, Tang XS, Khademhosseini A, Small 2016, 12, 3677. [PubMed: 27254107]

[109]. Annabi N, Shin SR, Tamayol A, Miscuglio M, Bakooshli MA, Assmann A, Mostafalu P, Sun J-Y, Mithieux S, Cheung L, Tang XS, Weiss AS, Khademhosseini A, Advanced materials (Deerfield Beach, Fla.) 2016, 28, 40.

[110]. Ryan AJ, Kearney CJ, Shen N, Khan U, Kelly AG, Probst C, Brauchle E, Biccai S, Garciarena CD, Vega-Mayoral V, Loskill P, Advanced Materials 2018, 30, 1706442.

[111]. Shin SR, Jung SM, Zalabany M, Kim K, Zorlutuna P, Kim SB, Nikkhah M, Khabiry M, Azize M, Kong J, Wan K-T, Palacios T, Dokmeci MR, Bae H, Tang XS, Khademhosseini A, ACS Nano 2013, 7, 2369. [PubMed: 23363247]

[112]. Ahadian S, Huyer LD, Estili M, Yee B, Smith N, Xu Z, Sun Y, Radisic M, Acta Biomater 2017, 52, 81. [PubMed: 27940161]

[113]. Lind JU, Busbee TA, Valentine AD, Pasqualini FS, Yuan H, Yadid M, Park S-J, Kotikian A, Nesmith AP, Campbell PH, Vlassak JJ, Lewis JA, Parker KK, Nature Materials 2017, 16, 303. [PubMed: 27775708]

[114]. Lee J, Manoharan V, Cheung L, Lee S, Cha BH, Newman P, Farzad R, Mehrotra S, Zhang K, Khan F, Ghaderi M, ACS nano 2019, 13, 12525. [PubMed: 31621284]

[115]. Wang Y, Zhang W, Huang L, Ito Y, Wang Z, Shi X, Wei Y, Jing X, Zhang P, Materials science & engineering. C, Materials for biological applications 2018, 90, 168. [PubMed: 29853080]

[116]. Liang S, Zhang Y, Wang H, Xu Z, Chen J, Bao R, Tan B, Cui Y, Fan G, Wang W, Wang W, Liu W, Advanced materials (Deerfield Beach, Fla.) 2018, 30, e1704235.

[117]. Roshanbinfar K, Vogt L, Greber B, Diecke S, Boccaccini AR, Scheibel T, Engel FB, Advanced Functional Materials 2018, 28, 1803951.

[118]. Dvir T, Timko BP, Brigham MD, Naik SR, Karajanagi SS, Levy O, Jin H, Parker KK, Langer R, Kohane DS, Nature nanotechnology 2011, 6, 720.

[119]. You JO, Rafat M, Ye GJ, Auguste DT, Nano letters 2011, 11, 3643. [PubMed: 21800912]

[120]. Song X, Wang X, Zhang J, Shen S, Yin W, Ye G, Wang L, Hou H, Qiu X, Biomaterials 2021, 273, 120811. [PubMed: 33882404]

[121]. He Y, Hou H, Wang S, Lin R, Wang L, Yu L, Qiu X, Bioactive Materials 2021, 6, 2000. [PubMed: 33426372]

[122]. Wang C, Chai Y, Wen X, Ai Y, Zhao H, Hu W, Yang X, Ding MY, Shi X, Liu Q, Liang Q, ACS Materials Letters 2021, 3, 1238.

[123]. Baheiraei N, Yeganeh H, Ai J, Gharibi R, Ebrahimi-Barough S, Azami M, Vahdat S, Baharvand H, Journal of biomedical materials research. Part A 2015, 103, 3179. [PubMed: 25765879]

[124]. Martins AM, Eng G, Caridade SG, Mano JF, Reis RL, Vunjak-Novakovic G, Biomacromolecules 2014, 15, 635. [PubMed: 24417502]

[125]. Spearman BS, Hodge AJ, Porter JL, Hardy JG, Davis ZD, Xu T, Zhang X, Schmidt CE, Hamilton MC, Lipke EA, Acta biomaterialia 2015, 28, 109. [PubMed: 26407651]

[126]. Chen S, Hsieh M-H, Li S-H, Wu J, Weisel RD, Chang Y, Sung H-W, Li R-K, Journal of Controlled Release 2020, 320, 73. [PubMed: 31958479]

[127]. He S, Song H, Wu J, Li SH, Weisel RD, Sung HW, Li J, Li RK, The Journal of heart and lung transplantation : the official publication of the International Society for Heart Transplantation 2018, 37, 912.

[128]. Zhou J, Chen J, Sun H, Qiu X, Mou Y, Liu Z, Zhao Y, Li X, Han Y, Duan C, Tang R, Wang C, Zhong W, Liu J, Luo Y, Mengqiu Xing M, Wang C, Sci Rep 2014, 4, 3733. [PubMed: 24429673]

[129]. Zhang C, Hsieh M-H, Wu S-Y, Li S-H, Wu J, Liu S-M, Wei H-J, Weisel RD, Sung H-W, Li R-K, Biomaterials 2020, 231, 119672. [PubMed: 31841751]

[130]. Li J, Fang W, Hao T, Dong D, Yang B, Yao F, Wang C, Composites Part B: Engineering 2020, 199, 108285.

[131]. Zhang J, Ma A, Shang L, Frontiers in physiology 2018, 9, 642. [PubMed: 29896120]

[132]. Jia C, Chen H, Wei M, Chen X, Zhang Y, Cao L, Yuan P, Wang F, Yang G, Ma J, Int J Nanomedicine 2017, 12, 4963. [PubMed: 28744126]
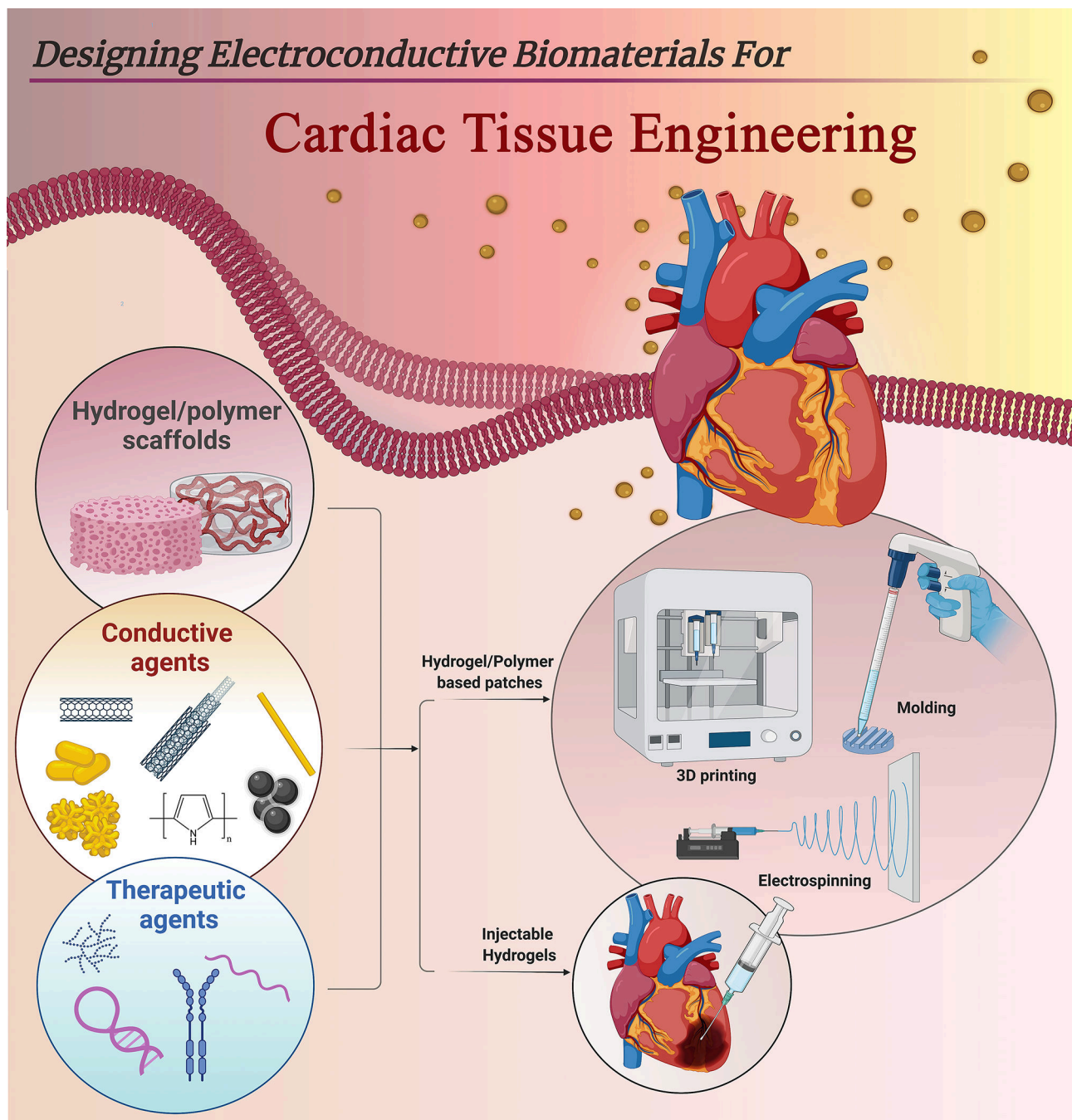
Figure 1. Electroconductive biomaterials designed for cardiac tissue engineering.
Examples of the biomaterials used for MI repair including: conductive agents such as
conductive polymers (e.g. PANI, PPy), gold- and carbon- based nanomaterials, ionic
liquids, conductive metal (oxide) NPs and nanowires, and therapeutic agents such as
siRNA, miRNA, growth factors, and small molecule inhibitors (e.g. 3i-1000), incorporated
in hydrogel/polymer scaffolds (e.g. GelMA, PEG, PCL); and strategies used to apply
biomaterials for cardiac tissue regeneration including: injectable hydrogels, and cardiac
patches produced by different methods such as molding, 3D printing, electrospinning,

and transplanted into the damaged area in the heart. Created with BioRender.com
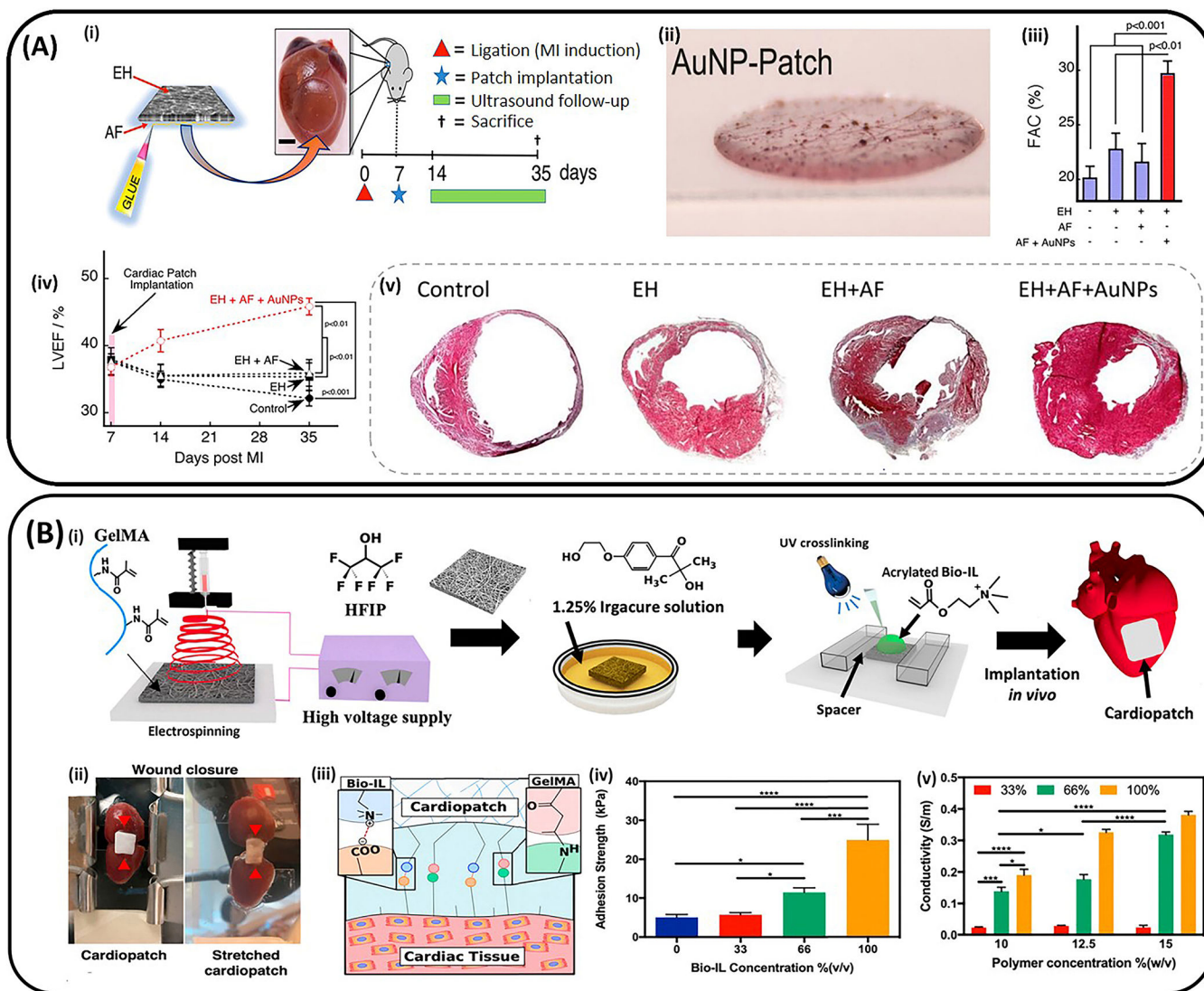
Abbreviations: 3D: three-dimensional; GelMA: gelatin methacryloyl; MI: myocardial infarction; miRNA; micro ribonucleic acid; NPs: nanoparticles; PANI: polyaniline; PCL: polycaprolactone; PEG: polyethylene glycol; PPy: polypyrrole; siRNA: small interfering ribonucleic acid.

Figure 2. Examples of electroconductive and electrospun cardiac patches used for MI repair.
(A) Engineering cardiac patches containing an AF layer and an EH layer; **(i)** Diagram summarizing the experimental procedure for *in vivo* implantation of the cardiac patches in an MI mouse heart model. The patches were glued to the left ventricular wall, using fibrin glue, **(ii)** Representative macro images of an AuNPs-containing cardiac patch, **(iii)** FAC during 35 days post-MI in mice treated with different samples, **(iv)** LVEF over time after treatment in MI mice (Implantation took place at day 7 post-MI). Experimental groups included nontreated animals (control), EH, EH + AF, and EH + AF-AuNPs, **(v)** Representative images of Masson-Trichrome staining of the mice hearts at day 28 post-implantation. Reproduced with permission.[47a] Copyright 2018, ACS applied materials & interfaces. **(B)** Engineering cardiac patches using electrospun GelMA fibrous sheet and Bio-IL; **(i)** Schematic illustration of the cardiac patch preparation, **(ii)** standard wound closure test using rat heart to test the adhesion strength of GelMA/Bio-IL cardiac patches, **(iii)** schematic illustration of interaction between cardiac tissue and engineered patches containing acrylated Bio-IL, **(iv)** quantification of the tissue adhesion strength of cardiac

patches fabricated with 10% (w/v) GelMA and varying concentrations of acrylated Bio-IL on heart tissue, **(v)** electrical conductivity of cardiac patches fabricated with varying GelMA and Bio-IL concentrations, demonstrating the electrical conductivity of patches increased by increasing acrylated Bio-IL concentrations. Reproduced with permission.[43a] Copyright 2019, Biomaterials.

Abbreviations: AF: aligned Col fiber; AuNPs: gold nanoparticles; Bio-IL: bio-ionic liquid; EH: elastic hydrogel; FAC: Fractional area change; GelMA: gelatin methacryloyl; LVEF: left ventricular ejection fraction; MI: myocardial infarction.
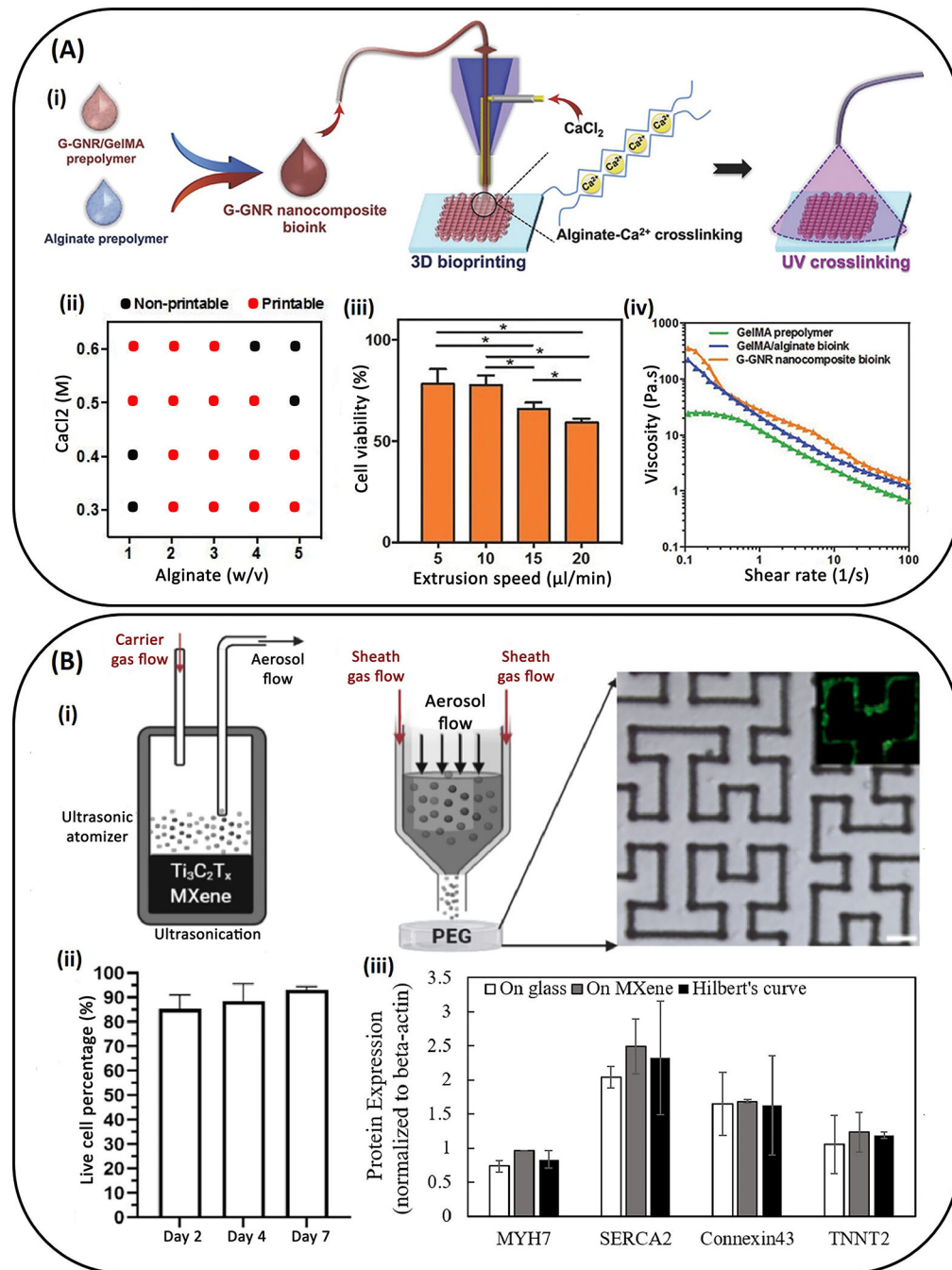
Figure 3. Examples of 3D printed electroconductive cardiac patches for MI repair.
(**A**) Engineering cardiac patches designed by using G-GNR/GelMA and Alg bioink; **(i)**
Schematic illustration of the 3D bioprinting process, **(ii)** Printability of different Alg
concentrations and different $CaCl_2$ concentrations (the concentrations of GelMA and G-
GNRs were kept as 7% (w/v) and 0.1 mg/mL, respectively), **(iii)** Live/dead assay of CFs
grown within G-GNR nanocomposite bioink printed constructs after printing with different
extrusion speed (*P<0.05) **(iv)** Rheological characterization of 7% (w/v) GelMA prepolymer
solution, GelMA/Alg bioink (7% (w/v) GelMA, 2% (w/v) Alg), and G-GNR nanocomposite

bioink (0.1 mg/mL G-GNR, 7% (w/v) GelMA, 2% (w/v) Alg). Reproduced with permission.
[59] Copyright 2017, Adv Funct Mater. **(B)** Engineering 3D printing conductive (Ti$_3$C$_2$T$_x$)
MXene in pre-designed patterns on PEG hydrogels using an aerosol jet printing; **(i)**
Schematic illustration of the 3D printing process as well as a representative Live/dead image
from the stem cell-derived CMs on Hilbert's curve pattern, **(ii)** Live cell percentage on days
2, 4 and 7 after seeding the Ti$_3$C$_2$Tx MXene-PEG composite hydrogels, **(iii)** Quantification
for the western blotting for the expressions of MYH7, SERCA2, GJA1, and TNNT2 proteins
(n = 2). Reproduced with permission.[37] Copyright 2020, Acta biomaterialia.

Abreviations: 3D: three-dimensional; Alg: alginate; CaCl$_2$: calcium chloride; CFs: cardiac
fibroblasts; CMs: cardiomyocytes; GelMA: gelatin methacryloyl; G-GNR/GelMA: GelMA
coated GNR incorporated GelMA; GJA1: gap junction alpha-1; GNR: gold nanorod;
MYH7: beta myosin heavy chain 7; PEG: polyethylene glycol; SERCA2: sarco/endo
plasmic reticulum calcium ATPase 2; Ti$_3$C$_2$T$_x$: titanium carbide; TNNT2: cardiac troponin T
type 2.
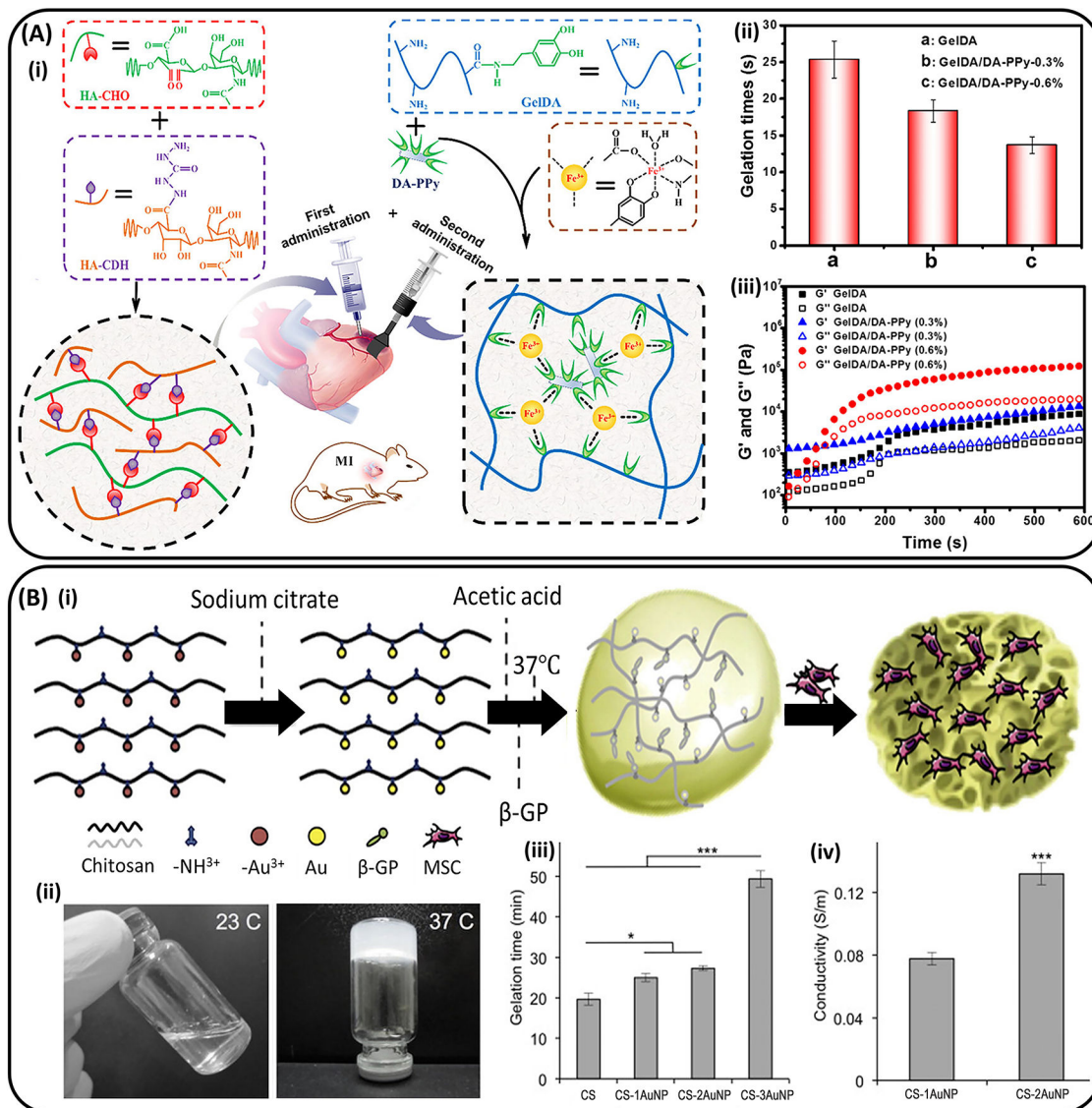
Figure 4. Examples of injectable and electroconductive hydrogels for cardiac tissue engineering.
(A) Coadministration of a conductive and adhesive hydrogel patch composed of GelDA and DA-PPy and an injectable hydrogel made of HA-CHO and HHA to the infarcted myocardium; **(i)** A schematic showing the preparation/applying process, **(ii)** Gelation time for hydrogels, **(iii)** Rheological analysis of hydrogels in a time-sweep mode at 37 °C. Reproduced with permission.[68] Copyright 2019, ACS applied materials & interfaces. **(B)** Engineering of a thermosensitive conductive hydrogel using CS and AuNPs; **(i)** Schematic illustration of the hydrogel preparation and *in vitro* seeding, **(ii)** Images of the CS solution (left) and gel (right) following a change in temperature, **(iii)** Gelation time assessment based on the test-tube-inverting method (n= 3, *P<0.05, ***P<0.001), **(iv)** Four-point probe conductivity of CS hydrogel that contained different concentrations of AuNPs (n = 3, ***P<0.001). AuNPs/CS (% w/w) = 0, 0.5, 1, and 1.5 in CS, CS-1AuNP, CS-2AuNP, and CS-3AuNP respectively. Reproduced with permission.[70] Copyright 2016, Materials science & engineering C. **Abbreviations:** AuNPs: gold nanoparticles; CS: chitosan; DA-

PPy: dopamine functionalized polypyrrole; GelDA: dopamine-gelatin; HA-CHO: oxidized sodium hyaluronic acid; HHA: hydrazided hyaluronic acid.
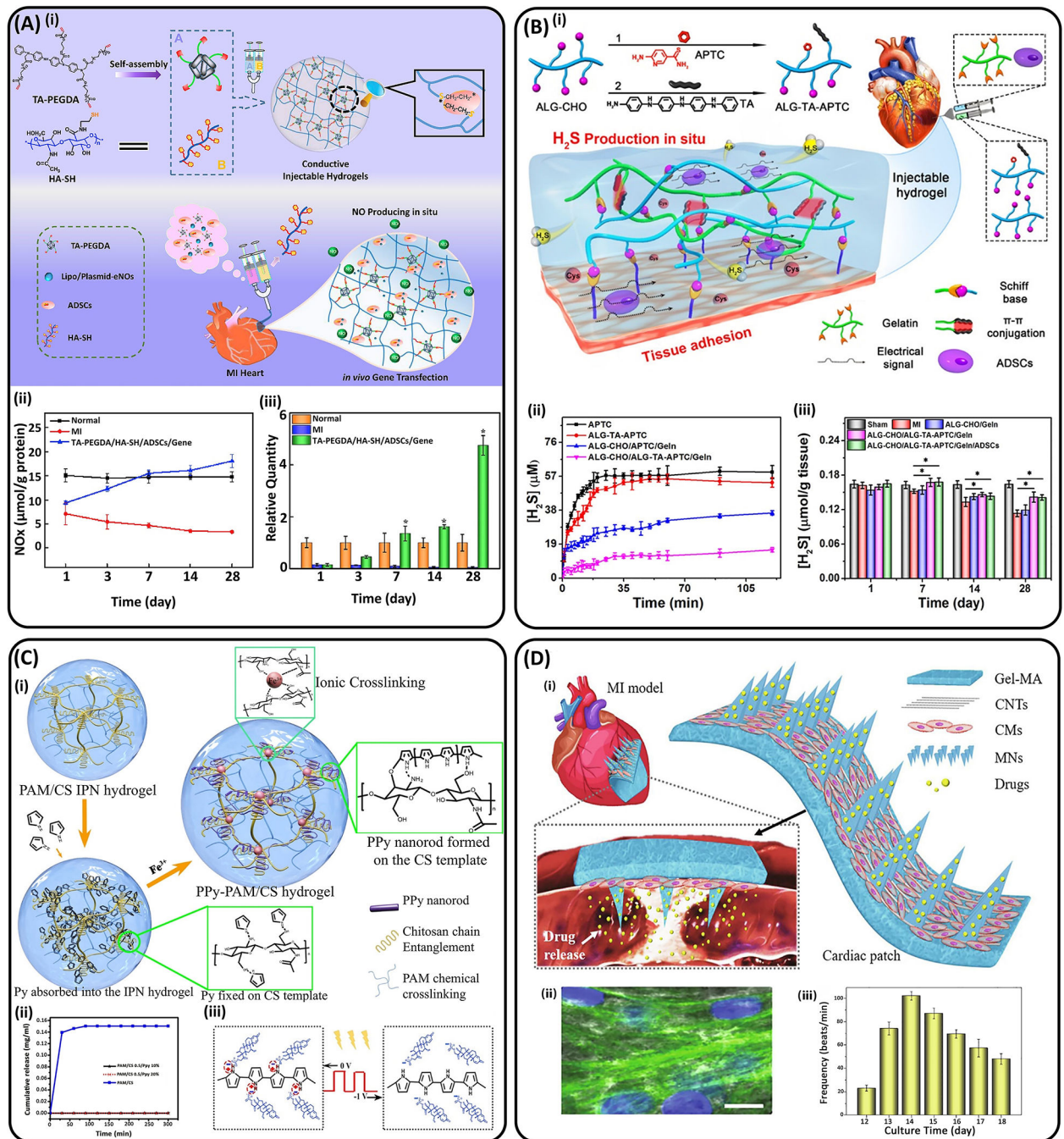
Figure 5. Examples of electroconductive patches for delivery of therapeutic agents for MI repair.
(**A**) An injectable conductive hydrogel developed for delivery of plasmid DNA-eNOs
and ADSCs for MI treatment; (**i**) Schematic demonstrating the conception to construct
a conductive injectable hydrogel, which was employed to load plasmid DNA-eNOs NPs
and ADSCs to treat myocardial infarction, (**ii**) NOx concentration in a 4 week time
period in normal and MI hearts, and in the MI hearts with TA-PEG/HA-SH/ADSCs/Gene
hydrogel treatment, (**iii**) The expression of mRNA of eNOs characterized by qRT-PCR
in a 4 week time period in normal and MI hearts, and in the MI hearts with TA-PEG/

HA-SH/ADSCs/Gene hydrogel treatment. Reproduced with permission.[88] Copyright 2018, Journal of Biomaterials. **(B)** Conductive H_2S-releasing hydrogel encapsulating ADSCs for myocardial infarction treatment**; (i)** A schematic presenting the ADSC-loaded conductive H_2S releasing hydrogel for damaged cardiac treatment; **(ii)** H_2S-releasing profile *in vitro*, **(iii)** sulfide concentration of the cardiac tissue in the MI area. Reproduced with permission. [89] Copyright 2019, ACS applied materials & interfaces. **(C)** PPy incorporated PAM/CS IPN loaded with dexamethasone; **(i)** A schematic of the synthesis process of PAM/CS IPN, **(ii)** the role of electrostimulation on the Dexamethasone release, **(iii)** Releasing of the dexamethasone by the redox process when the negative potential was applied. Reproduced with permission.[93] Copyright 2018, ACS applied materials & interfaces. **(D)** Engineering of CNTs integrated MN patch; **(i)** Schematic illustration of applying the engineered patches on the infarcted myocardium, **(ii)** Confocal laser scanning microscope image of the aligned hiPSC-derived CMs cultured on the conductive MN array patch (Scale bars: 20 μm), **(iii)** The beating performance of the cells cultured on the conductive patch. Reproduced with permission.[94] Copyright 2021, Chemical Engineering Journal. **Abbreviations:** ADSCs: adipose-derived stem cells; CNTs: carbon nanotubes; DNA-eNOs: deoxyribonucleic acid-endothelial nitric oxide synthase; HA-SH: Thiol modified hyaluronic acid; H_2S: hydrogen sulfide; hiPSC-derived CMs: human induced pluripotent stem cell derived cardiomyocytes; MI: myocardial infarction; MN: integrated microneedle; NPs: Nanoparticles; PAM/CS IPN: polyacrylamide/chitosan interpenetrating hydrogels; PEGDA: poly(ethylene glycol) diacrylate; PPy: polypyrrole; qRT-PCR: Quantitative Reverse Transcription-Polymerase Chain Reaction; TA: Tetraaniline.

Table 1.

A summary of electroconductive cardiac patches for cardiac tissue regeneration

Fabrication method	Biomaterial	Conductivity (S/m)	Mechanical properties	Application	Outcome	Ref
Electrospinning	Col+ AgNPs & Col+ AuNPs	AgNPs ~ 0.35 $\times 10^{-6}$ AuNPs ~ 0.8 $\times 10^{-6}$	Young's modulus~ 20.1 kPa	*In vitro*/ *In vivo (mouse MI model)*	Increase in Cx43 expression in NRCMs cultured under electrical stimulation; Increase in blood vessel density; Decrease of scar size	[47a]
	PES+ CPSA+ PANI	0.057	Tensile strength~ 3.5 MPa	*In vitro*	Increase in the number of *TNNT2*; Increase in the derivation of CMs from human CVD-iPSCs; Induction of pluripotent stem cells	[97]
	EB+ PLGA+ PANI	0.31	Young's modulus~ 91.7 MPa	*In vitro*	Synchronization of beating rates among NRCMs clusters via an electrical stimulation; Improvement of heart function	[98]
	Col+ HA+ PANI	0.2	Tensile strength ~ 10 MPa; Tensile strain~ 3.2%; Young's modulus~ 4 MPa	*In vitro*	Increase in the Cx43 expression in CMs; Significant improvement in the attachment, and function of hiPSC-derived CMs	[99]
	PLGA+ PPy	NA	NA	*In vitro*	Direct electrical and mechanical stimulation to the hiPSC; No cytotoxic effects on the hiPSC; Increase in expression of cardiac markers	[100]
	GelMA+ Acrylated Bio-IL	0.190	Elastic modulus~ 145.50 kPa; Tensile strength~ 64.59 kPa	*In vitro*/ *In vivo (mouse MI model)*	Mechanical and conductive properties similar to the native myocardium; Adherence to murine myocardium; Over-expression of Cx43; No cytotoxic effects on the co-cultures of CMs and CFs	[43a]
	PLCL+ Gelatin+ MEL	0.0259	Young's modulus~ 7.1 MPa; Tensile strength~ 0.95 MPa	*In vitro*	Improvement in human CMs proliferation and the expression of Cx43	[47c]
	PCL+ SF+ CNT	(6.5– 8.1) $\times 10^{-5}$	Young's modulus~ 110 MPa	*In vitro*	Control of cellular orientation; Improvement in CMs maturation; Control of cellular orientation; Induction of cellular orientation, maturation, and anisotropy	[101]
	PELA+ CNT	3.74	Young's modulus~ 70.8 MPa	*In vitro*	Improvement in NRCMs growth	[102]
	PGS+ Gelatin+ CNT	NA	Toughness~ 1948.7 KJm^{-3}; Tensile strength~ 1.35 MPa	*In vitro*	Improvement in fiber alignment, electrical conductivity, and mechanical toughness; Improvement in NRCMs alignment and contractile activities	[27a]
	Silk+ GO+ MoS$_2$	2×10^{-7}	Tensile strength~ 3.74 MPa	*In vitro*	Improvement in the maturity and upregulation of cardiac functional genes in hiPSCs transfected with TBX-18 gene	[103]

Fabrication method	Biomaterial	Conductivity (S/m)	Mechanical properties	Application	Outcome	Ref
	β-PVDF nanocomposite	NA	Tensile strength~ 88 MPa; Tensile strain~ 80%	*In vitro*	Improvement in NRCMs adherence and differentiation	[104]
	PPy+ SF	NA	Young's modulus~ 1.437 MPa	*In vitro*	Improvement in the elongation of NRCMs; Increase in the contraction of hiPSC-derived CMs	[105]
3D printing	PEG+ $Ti_3C_2T_x$ MXene	1.1×10^4	Elastic modulus~ 144.5 kPa	*In vitro*	Increase in hiPSC-derived CMs alignment; Synchronous beating improvement; Conduction velocity improvement	[37]
	Cellulose+ SWCNT	43	Tensile strength~ 103 MPa; Tensile strain~ 18.7%; Young's modulus~ 1.26 GPa	*In vivo (canine model)*	Restoration of conduction	[39]
	dECM+ rGO	0.0005 – 3.07	Compressive modulus~ 17.5 kPa	*In vitro*	Enhancement of gene expression regulating contractile function; Improvement in calcium handling capabilities	[106]
	Nanocellulose+ PGS+ PPy	3.4	Young's modulus~ 0.6 MPa	*In vitro*	Effective integration of rat cardiomyoblasts with the biomaterial	[47b]
	GelMA+ Alg+ G-GNR	NA	Young's modulus~ 4.7 kPa	*In vitro*	Improvement in cell adhesion and organization; Improvement in synchronized contraction of NRCMs	[59]
Molding	Col+ rGO	$\sim 10^{-4}$	Tensile strength~ 162 kPa	*In vitro/ In vivo (mouse subcutaneous model)*	Improvement in angiogenesis; No toxic effects on HUVECs	[107]
	GelMA+ rGO	NA	Young's modulus~ 22.6 kPa	*In vitro*	Strong contractility and fast spontaneous beating rate of NRCMs	[108]
	MeTro+ GO	NA	Elastic modulus~ 19.3 kPa	*In vitro/ In vivo (rat subcutaneous model)*	Improvement in local and nanoscale electrical conductivity; Induction cell-cell signaling of NRCMs	[109]
	Col+ Graphene	0.1–0.7	NA	*In vitro*	Improved CF functions; Inhibition of bacterial attachment; Improvement in NRCMs metabolic activity	[110]
	GelMA+ CNT	NA	Compression modulus~ 32 kPa; Elastic modulus~ 20 kPa	*In vitro*	Excellent mechanical integrity; Improved electrophysiological functions; No CNT cytotoxic effect on NRCMs	[111]
	124 Polymer+ MWCNT	0.08×10^{-3}	Bulk modulus~ 2.2 Mpa; Surface modulus~ 3.3 Mpa; Toughness~ 76 $MJ\ m^{-3}$	*In vitro*	Improvement in excitation threshold; Insignificant cytotoxic effect on NRCMs	[112]

Fabrication method	Biomaterial	Conductivity (S/m)	Mechanical properties	Application	Outcome	Ref
	GelMA+ CNT	NA	Tensile strength~ 0.065 MPa;	*In vitro/ In vivo (mouse MI model)*	Induction the orientation growth of hiPSC- derived CMs; Adherence to the injured part; Increase in the infarct wall thickness and improvement in the function recovery	[94]
	Col+ CNT	NA	Young's modulus~ 8.8 MPa	*In vitro*	Improvement in hiPSC-derived CMs alignment; Improvement in the functionality of cardiac constructs	[113]
	GelMA+ CNT or GO or rGO	NA	Elastic modulus~ 16.8 kPa (using CNT), 47.9 kPa (using GO), 59.8 kPa (using rGO)	*In vitro*	Higher expression of cardiac markers (sarcomeric α-actin, Cx43, and troponin I); Promotion of cardiac cell morphology and contractility of NRCMs	[114]
	CS+ PANI	~1	Tensile strength~ 1.53 MPa; Tensile strain~ 96%	*In vitro/ In vivo (rat MI model)*	No detrimental effect on the cardiac electrophysiology; Tunable mechanical and conductive properties; Cytocompatible with NRCMs	[46]
	PLA+ PAP	$10^{-3} - 10^{-4}$	NA	*In vitro*	Improvement in electronic signals transferring between rat cardiac myoblast cells	[115]
	HPAE+ Py + Fe^{+3} + Gelatin	0.0651	Adhesive strength~ 22.2 kPa	*In vitro/ In vivo (rat MI model)*	Increase in the transmission of electrophysiological signals; Reconstruction improvement of cardiac function; Revascularization improvement	[116]
	Col+ Alg+ PEDOT:PSS	0.35	NA	*In vitro*	Improvement in sarcomere organization; Improvement in Cx43 expression; Improvement in maturation and beating properties of hiPS– derived CMs; Improvement in beating frequency; Increase in speed of contraction; Large contraction amplitude	[117]
	Alg+ AuNWs	NA	NA	*In vitro*	Improvement in the electrical communication between adjacent NRCMs; Improved alignment of tissues grown; Participation of higher levels of protein expression in the muscle contraction and electrical coupling	[118]
	Thiol-HEMA+ AuNPs	15.3	Young's modulus~ 0.6 MPa	*In vitro*	Increase in expression of Cx43 in NRCMs	[119]
	GelMA+ GNR	NA	Young's modulus~ 1.3 kPa	*In vitro*	Fast and synchronous electrical signal propagation; Rhythmic contraction of the NRCMs on GelMA/GNR	[45]
	Gelatin +OA +butene-modified PAA	3.53	Tensile strain~ 500%; Compressive strain~ 85%; Tensile strength~ 37 kPa	*In vitro/ In vivo (rat MI model)*	Suppression of cardiac fibrosis; Restoration of heart function; Induction of cellular orientation and elongation using NRCMs	[120]

Fabrication method	Biomaterial	Conductivity (S/m)	Mechanical properties	Application	Outcome	Ref
	PTC	0.005– 0.16	Young's modulus~ 0.59 MPa	*In vitro/ In vivo (rat MI model)*	Improvement in maturation and spontaneous contraction of NRCMs; Enhancement of cardiac function	[121]
	PPy nanotube+ sodium Alg+ PAM	4500	Young's modulus~ 4–40 kPa	*Ex vivo*	Alignment of conductive PPy nanotubes using simple stretch-induced strategy; Increase in the CMs elongation and stable directional transmission of electric signals; Enhancement in the mitigation of MI in rats	[122]
	PU+ PCL+ AP	10^{-3}	Compression modulus~ 4.1 MPa; Compression strength~ 1.3 MPa	*In vitro*	NRCMs adhesion and growth and expression of the cardiac genes (troponin- T) and cytoskeleton alignment (actinin-4)	[123]
Other methods (e.g. chemical vapor deposition, precipitation, …)	PEG+ Graphene	NA	NA	*In vitro*	Structural property enhancement in myofibrils and sarcomeres; Significant increase in the expression of cell-cell coupling and calcium handling proteins	[42a]
	CS+ Carbon	0.25	Elastic modulus~ 28.1 kPa	*In vitro*	Increase in expression of cardiac-specific genes involved in muscle contraction and electrical coupling; Enhancement in transmission of electrical signals between the NRCMs	[124]
	PCL +PPy	NA	Elastic modulus~ 0.93 GPa; Stiffness~ 0.071 GPa	*In vitro*	Enhancement in functional properties and maturation of CMs	[125]
	Gelfoam+ PAMB	0.019	Young's modulus~ 1 kPa; Tensile strength~ 2 kPa; Tensile strain~ 180%	*In vitro/ In vivo (rat MI model)*	Improvement in electrical activity in the fibrotic tissue; Improvement in electrical impulse propagation; Synchronization of NRCM contraction across the scar region	[126]
	CS+ Gelfoam+ PPy	~ 0.0125	Tensile strength~ 20 kPa;	*In vitro/ In vivo (rat MI model)*	Increase in Ca^{2+} transient velocity of NRCMs cultured on cardiac patches; No pathological arrhythmias after patch implantation	[127]
	Gelatin+ SWCNTs	~ 0.7×10^{-4}	NA	*In vitro/ In vivo (rat MI model)*	Increase in the expression of TNNT2/sarcomeric actinin and Cx43 using NRCMs	[128]

Abbreviations: 124 polymer: poly(octamethylene maleate (anhydride) 1,2,4-butanetricarboxylate; Ag: Silver; Alg: Alginate; AP: Aniline pentamer; Au: Gold; AuNWs: Gold nanowires; Bio-IL: Bio-ionic liquid; β-PVDF: Beta-polyvinylidene fluoride; CF: Cardiac fibroblast; CS: Chitosan; CMs: Cardiomyocytes; CNT: Carbon nanotube; Col: Collagen; CPSA: Camphor-10-sulfonic acid (β); CVD-iPSCs: Cardiovascular disease-specific induced pluripotent stem cells; Cx43: Connexin-43; dECM: Decellularized porcine myocardial extracellular matrix; GelMA: Gelatin methacryloyl; G-GNR: GelMA-coated GNR; GNR: Gold nanorod; GO: Graphene oxide; HA: Hyaluronic acid; HPAE: Highly branched poly(β-amino ester); iPSC: Induced pluripotent stem cells; hiPSC: Human-induced pluripotent stem cell; HUVECs: human umbilical vein endothelial cells; MEL: Melanin; MeTro: Methacryloyl-substituted recombinant human tropoelastin; MI: Myocardial infarction; MoS_2: molybdenum disulfide; MWCNT: Multi-walled carbon nanotube; NA: Not mentioned; NPs: Nanoparticles; NRCM: Neonatal rat cardiomyocyte; OA: oxidized alginate; PAA: Poly acrylic acid; PAM: Polyacrylamide; PAMB: Poly-3-amino-4-methoxybenzoic acid; PANI: polyaniline; PAP: PLA-b-AP-b-PLA triblock copolymer; PCL: Polycaprolactone; PEDOT: PSS: Poly(3,4-ethylenedioxythiophene) polystyrene sulfonate; PEG: Polyethylene glycol; PELA: Poly(ethylene glycol)-poly(D,L-lactide) copolymers; PES: Polyetersulfone; PGS: Poly(glycerol sebacate); PLA: Poly (L-lactide); PLCL: Poly(L-lactide-co-ε-caprolactone); PLGA: Poly(lactic- co -glycolic acid); PMMA: poly(methyl methacrylate); PPy:

Polypyrrole; PTC: PPy modified tunic cellulose; PU: Polyurethane; Py: Pyrrole; rGO; Reduced graphene oxide; SF: Silk fibroin; SWCNT: Single-walled carbon nanotube; Thiol-HEMA: Thiol-2- hydroxyethyl methacrylate; Ti: Titanium; $Ti_3C_2T_x$ MXene: Titanium carbide; TNNT2: cardiac troponin T type 2.

Author Manuscript

Author Manuscript

Author Manuscript

Author Manuscript

Table 2.

A summary of electroconductive injectable hydrogels for cardiac tissue regeneration

Biomaterial	Conductivity (S/m)	Application	Outcome	Ref
GelMA+ PEI+ fGO+ VEGF	NA	*In vitro/ In vivo*	Reduced infarcted size; Increase in myocardial capillary density and cardiac performance	[63a]
CS-AuNPs+ CS + β-GP	0.16	*In vitro*	Enhancement in the properties of myocardial constructs; Support of viability, metabolism, migration, and proliferation of MSCs along with the development of uniform cellular constructs	[70]
PEGDA+ MEL+ HA-SH+ GO	0.0284	*In vitro/ In vivo*	A significant increase in α-SMA and Cx43 expression; Improvement in the transmission of mechanical and electrical signals; A significant improvement of heart functions	[19e]
PEGDA-TA+ HA-SH	0.0232	*In vitro/ In vivo*	Increase in expression of eNOs; Upregulation of pro-angiogenic growth factors and myocardium related mRNA; A significant improvement of heart functions	[88]
CS+ PPy	~ 0.023	*In vitro/ In vivo*	Improvement of heart function	[67]
ECM+ MWCNT	1.5	*In vitro*	CMs proliferation; A significant increase in Cx43 expression	[72]
PAMB-Gelatin	NA	*In vitro/ In vivo*	Improvement in electrical impulse propagation; Synchronization of heart contraction; Preservation of the ventricular function; Reduction of cardiac arrhythmia	[129]
GelDA/DA-PPy+ HA-CHO-HHA	0.0001–0.028	*In vivo*	Attachment onto the myocardium surface; Improvement in cardiac function after MI injury	[68]

Abbreviations: Au: Gold; CS: Chitosan; CS-AuNPs: Chitosan-stabilized gold nanoparticles; Cx43: Connexin-43; DA-PPy: Dopamine-modified polypyrrole; ECM: extracellular matrix; eNOs: Endothelial nitric oxide synthase; fGO: functionalized GO nanosheets; GelDA: Gelatin-dopamine; GelMA: Gelatin methacryloyl; GO: Graphene oxide; HA: Hyaluronic acid; HA-CHO: Oxidized sodium hyaluronic acid; HA-SH: Thiol modified hyaluronic acid; HHA: Hydrazided hyaluronic acid; MEL: Melanin; MI: Myocardial infarction; mRNA: Messenger ribonucleuc acid; MSCs: Mesenchymal stem cells; MWCNT: Multi-walled carbon nanotube; NA: Not mentioned; PAMB: Poly-3-amino-4-methoxybenzoic acid; PEGDA: Poly(ethylene glycol) diacrylate; PPy: Polypyrrole; TA: Tetraaniline; VEGF: Vascular endothelial growth factor; α-SMA: α-Smooth muscle actin; β-GP: β-glycerophosphate disodium salt solution.

Table 3.

Recent electroconductive materials designed for delivery of different types of therapeutic agents to the heart

Biomaterial	Therapeutic agent	Outcome	Ref
PGS-Puppy-triethoxysilane-porous silicon NPs	3i-1000	Appropriate electrical conductivity and controlled drug release for improvement of cardiac myoblast cell attachment and cytotoxicity	[83]
Oxidized Alg+ TA+ ADSCs	H_2S	Adhesive property, upregulation of cardiac-related mRNA (e.g. Cx43, α-SMA, and cTnT) and angiogenic factors (e.g. VEGFA and Ang-1) and downregulation of inflammatory factors (e.g. tumor necrosis factor-α)	[89]
TA+ PEGDA+ HA-SH+ ADSCs	Plasmid DNA encoding eNOs	Equivalent myocardial conductivity; Upregulation of pro-angiogenic growth factors, and myocardium-related mRNA; Reduced infarction size, less fibrosis area, and higher vessel density	[88]
GelMA+ PEI+ fGO	$VEGF_{165}$ pro-angiogenic gene	Reduced infarcted size; Increase in myocardial capillary density and cardiac performance	[63a]
GO nanosheets	IL-4 plasmid DNA	Increased M1 to M2 macrophage polarization and accelerated cardiac repair	[81]
GelMA-CNT MN patch	VEGF, IL-10	Adhesive property to the heart and controlled release of encapsulated drugs; Stimulate the contraction of CMs	[94]
Gelatin scaffold	Glutathione grafted to the carboxyl-capped aniline pentamer	High conductivity and antioxidant activity which removes intracellular ROS and decreases oxidative stress damage in adipose-derived stem cells	[130]
Oxidized nanocellulose+ PGS+ PPy 3D-printed patches	3i-1000 and curcumin	Improved regeneration of myocardium	[84]
PPy nanorods loaded PAM/CS hydrogel	Dexamethasone	Controlled drug release, depending on the PPy content, and stimulation voltage; Improved C2C12 cell activity under electrostimulation	[93]
AuNPs	Simdax	Cardioprotective effects in rats with heart failure	[131]
AuNPs	miR155	Treatment of diabetic cardiomyopathy; Increase anti-inflammatory macrophages and reduce the inflammation and cell apoptosis; Restoration of cardiac function	[132]

Abbreviations: ADSC: Adipose-tissue derived stem cell; Alg: Alginate; Ang-1: Angiopoietin 1; Au: Gold; AuNPs:Gold nanoparticles; CNT: Carbon nanotube; cTnT: Cardiac troponin T; Cx43: Connexin-43; DNA: Deoxyribonucleic acid; eNOs: Endothelial nitric oxide synthase; fGO: functionalized GO nanosheets; GelMA: Gelatin methacryloyl; H_2S: Hydrogen sulfide; HA-SH: Thiol modified hyaluronic acid; IL-10: Interleukin-10; IL-4: Interleukin-4; miR155: MicroRNA155; MN: Microneedle; mRNA: Messenger ribonucleuc acid; NPs: Nanoparticles; PAM: Polyacrylamide; PEGDA: Poly(ethylene glycol) diacrylate; PEI: Polyethylenimine: PGS: Poly(glycerol sebacate); PPy: Polypyrrole; RNA: Ribonucleuc acid; Simdax: Levosimendan; TA: Tetraaniline; VEGFA: Vascular Endothelial Growth Factor A; α-SMA: α-Smooth muscle actin.